



IN THE UNITED STATES PATENT AND TRADEMARK OFFICE

Applicant: Roger E. Welser, Paul M. DeLuca and Noren Pan

Application No.: 10/824,697 Group: 2813

Filed: April 14, 2004 Examiner: Rodgers, Colleen E.

Confirmation No.: 6799

For: BIPOLAR TRANSISTOR WITH LATTICE MATCHED BASE LAYER

CERTIFICATE OF MAILING OR TRANSMISSION	
I hereby certify that this correspondence is being deposited with the United States Postal Service with sufficient postage as First Class Mail in an envelope addressed to Commissioner for Patents, P.O. Box 1450, Alexandria, VA 22313-1450, or is being facsimile transmitted to the United States Patent and Trademark Office on:	
9-7-06	Mary J. Dawson
Date	Signature
MARY J. DAWSON	
Typed or printed name of person signing certificate	

DECLARATION OF ROGER E. WELSER, Ph.D. UNDER 37 C.F.R. § 1.131

Mail Stop RCE
Commissioner for Patents
P.O. Box 1450
Alexandria, VA 22313-1450

I, Roger E. Welser, Ph.D. of Providence, RI declare as follows:

1. I am a co-inventor of the subject patent application, US Patent Application No. 10/824,697 entitled "Bipolar Transistor with Lattice Matched Base Layer."
2. I have read U.S. Patent Application No. 10/824,697 and the Office Action mailed March 29, 2006. I understand the application, the pending Office Action and the issues relating to patentability presented by the Examiner in the Office Action for the invention claimed in the patent application.

PEW
9/8/06

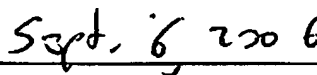
3. I have read and understand, U.S. 6,765,242 B1 to Chang, *et al.* (hereinafter "Chang, *et al.*") which was filed April 11, 2000 and patented July 20, 2004.
4. I hereby state that the invention described and claimed in the above-referenced application was reduced to practice prior to April 11, 2000, the filing date of Chang, *et al.* The reduction to practice prior to April 11, 2000 is evidenced by the attached Exhibits A and B.
 - A. Exhibit A is a redacted copy of a Phase I Report, prepared prior to April 11, 2000, for the Small Business Technology Transfer (STTR) Program. As described in the Abstract on page 1, a process for growing heavily doped p-type GaInAsN was developed during the Phase I effort. For example, incorporation greater than $1\text{E}19\text{ cm}^{-3}$ levels of carbon (C) and incorporation of nitrogen (N) in GaInAs materials were achieved, as shown in Figure 3 on page 7 ($2.5\text{E}19\text{ cm}^{-3}$ of C); 1st full paragraph on page 9 ($2\text{E}19\text{ cm}^{-3}$ of C and $1\text{E}18\text{ cm}^{-3}$ of N) and Figure 6 on page 10; pages 13 through 16 ($8.4\text{E}18\text{ cm}^{-3}$ of N and $3.5 - 6.9\text{E}19\text{ cm}^{-3}$ of C). Also, as described, for example, in the Abstract on page 1, InGaP/GaInAsN heterojunction transistors (HBTs) with a base sheet resistance of 279 ohms/square and peak dc current gain greater than 30 were achieved during the Phase I effort, and such HBTs exhibited over an 11 meV reduction in turn-on voltage.
 - B. Exhibit B is a redacted copy of a Phase II proposal, prepared prior to April 11, 2000, laying out research proposals for improving the invention described in Exhibit A, for example, by improving the process for growing heavily doped p-type GaInAsN and by improving device performance in GaInAsN-based HBTs. Throughout the document, Exhibit B confirms the results achieved during the Phase I effort, e.g., growth of a heavily doped p-type GaInAsN as described in Section 4, A, above.

Raw
9/6/06

5. I further declare that all statements made herein of my own knowledge are true and that all statements made on information or belief are believed to be true; and further that these statements are made with the knowledge that willful false statements and the like so made are punishable by fine or imprisonment, or both, under § 1001 of Title 18 of the United States Code, and that such willful false statements, if made, may jeopardize the validity of the application or any patent issuing thereon.



Roger E. Welser, Ph.D.



Date

REPORT DOCUMENTATION PAGE

Form Approved
OMB No. 0704-0188

Public reporting burden for this collection of information is estimated to average 1 hour per response, including the time for reviewing instructions, searching existing data sources, gathering and maintaining the data needed, and completing and reviewing the collection of information. Send comments regarding this burden estimate or any other aspect of this collection of information, including suggestions for reducing this burden, to Washington Headquarters Services, Directorate for Information Operations and Reports, 1215 Jefferson Davis Highway, Suite 1204, Arlington, VA 22202-4302, and the Office of Management and Budget, Paperwork Reduction Project (0704-0188), Washington, DC 20503.

1. AGENCY USE ONLY (Leave Blank)		2. REPORT DATE		3. REPORT TYPE AND DATES COVERED Final Report	
4. TITLE AND SUBTITLE Low-Voltage GaAs-Based HBTs				5. FUNDING NUMBERS	
6. AUTHOR(S) Roger E. Welser					
7. PERFORMING ORGANIZATION NAME(S) AND ADDRESS(ES) Kopin Corporation 695 Myles Standish Blvd. Taunton, MA 02780				8. PERFORMING ORGANIZATION REPORT NUMBER	
9. SPONSORING/MONITORING AGENCY NAME(S) AND ADDRESS(ES) AFRL/SNO Bldg. 620 2241 Avionics Circle, Ste. 18 Wright Patterson AFB, OH 45433-7320				10. SPONSORING/MONITORING AGENCY REPORT NUMBER	
11. SUPPLEMENTARY NOTES					
12a. DISTRIBUTION/AVAILABILITY STATEMENT				12b. DISTRIBUTION CODE	
13. ABSTRACT (Maximum 200 words) During this Phase I STTR program, Kopin Corporation has demonstrated the feasibility of lowering the turn-on voltage of InGaP/GaAs heterojunction bipolar transistors (HBTs) by incorporating both In and N into the base layer of the HBT structure. Numerous laboratories have demonstrated that the energy-gap of GaInAs drops substantially with the addition of small amounts of N. Moreover, because N pushes the lattice constant in the opposite direction from In, GaInAsN alloys can be grown closely lattice-matched to GaAs. During our Phase I effort, we developed a proprietary growth process for synthesizing heavily doped p-type GaInAsN which is entirely compatible with high volume manufacturing. InGaP/GaInAsN HBTs with a base sheet resistance of 279 Ω/\square and peak dc current gain greater than 30 exhibit over an 11 meV reduction in turn-on voltage (V_{be} @ $J_c = 1.78 \text{ A/cm}^2$). Phase II work will focus on increasing the C, N, and In concentrations of the GaInAsN base layer material while at the same time improving the minority carrier lifetime. Initial studies at Kopin and Yale University have proven the feasibility of simultaneously incorporating greater than $1 \times 10^{19} \text{ cm}^{-3}$ levels of C and N in $\text{Ga}_{0.96}\text{In}_{0.04}\text{As}$.					
14. SUBJECT TERMS Heterojunction Bipolar Transistor Microwave Communication GaInAsN MOCVD				15. NUMBER OF PAGES 25	
				16. PRICE CODE	
17. SECURITY CLASSIFICATION OF REPORT UNCLASSIFIED	18. SECURITY CLASSIFICATION OF THIS PAGE UNCLASSIFIED	19. SECURITY CLASSIFICATION OF ABSTRACT UNCLASSIFIED	20. LIMITATION OF ABSTRACT		

EXHIBIT

A

REF D

Standard Form 298 (Rev. 2-89)
Prescribed by ANSI Std. Z39-18

Motivation and Objectives

The increasing trend toward lower supply voltages in many communication systems has spurred a great interest in material systems enabling HBTs with low turn-on voltages, high power added efficiency, high linearity, and high output powers. Although InP-based HBTs offer low turn-on voltages with respectable power performance, the process and growth technology needs substantial work to reach volume production. The difficulty of C-doping InGaAs lattice-matched to InP and the unavailability of large area substrates for manufacturing also limit the potential of InP-based HBTs. At the laboratory level, SiGe-based HBTs have demonstrated reasonable RF performance and low turn on-voltages, but good power handling capabilities, long-term reliability, and volume manufacturability still need to be proven. The potential payoff would be tremendous if GaAs-based HBTs can be engineered to realize low turn-on voltages.

The turn-on voltage of an HBT is fundamentally limited by the energy-gap of the base layer (E_{gb}). In the absence of series resistance and conduction band spike effects, the base-emitter voltage (V_{be}) for a given collector current density (J_c) is:

$$V_{be} = E_{gb}/q - (kT/q) \ln[(qD_n N_c N_v)/(p_b w_b J_c)] \quad (1)$$

where p_b and w_b are the base doping and width, D_n is the diffusion coefficient, and N_c and N_v are the effective density of states in the conduction and valence bands in the base layer [1].

Historically, there have been no materials available which both have a smaller energy-gap than GaAs and are lattice-matched to GaAs substrates. Recently, there have been numerous reports concerning GaAs and related compounds doped with small amounts of N [2-4]. Such GaAsN alloys have a number of interesting properties, not the least of which is a very large reduction in energy gap with the addition of small amounts of N. At the beginning of our Phase I effort, we planned to limit our attention to adding small amounts of N to C-doped GaAs. However, part way through the program, we discovered we could add In as well and still maintain a reasonable doping level ($>2 \times 10^{19} \text{ cm}^{-3}$). In and N push the lattice constant in opposite directions, and both lower the energy-gap of GaAs. Thus, by adding both In and N to GaAs, it is possible to dramatically lower the energy-gap while maintaining a lattice-matched film (Figure 1). Several groups have already incorporated such GaInAsN alloys into device structures which take advantage of the lower energy-gap, including fiber-optic wavelength laser diodes [5] and solar cells [6]. The objective of this STTR program has been to study the feasibility of synthesizing GaInAsN films with heavy p-type doping for incorporation into the base layer of GaAs-based HBTs. If successful, it may be possible to realize microwave devices with the speeds associated with III-V materials at Si-like turn-on voltages.

While a lower turn-on voltage is the key motivation for adding N and In to the base layer of GaAs-based HBTs, a number of secondary benefits to device performance have also been identified. The anticipated benefits associated with using low energy-gap GaInAsN base layers in a conventional GaAs-based HBT device structure include:

- **Lower turn-on voltage:** The addition of just 2% of N and 6% of In to GaAs can lower the energy-gap to well below that of Si (1.12 eV) and yet maintain lattice-matching to GaAs. By reducing the base layer energy-gap from 1.42 (GaAs) to 1.12 eV, the HBT turn-on voltage (V_{be} @ 100 μA) is expected to shift from 1.12 V to 0.80 V.

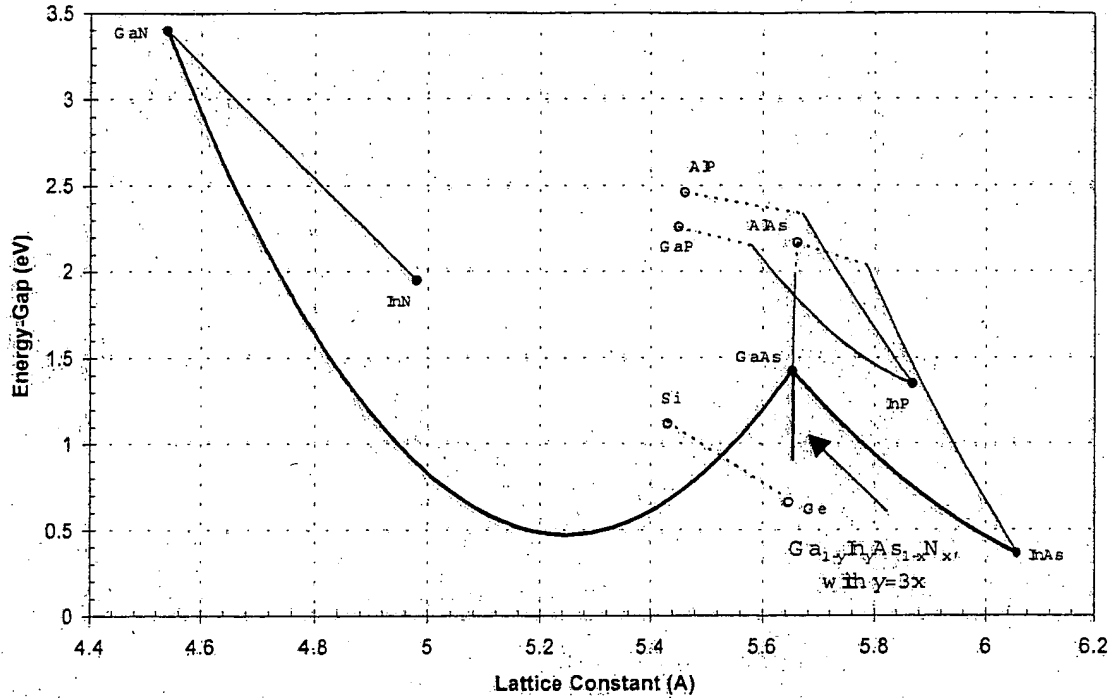


Figure 1: Energy-gap vs. lattice constant for common III-V semiconductors including GaAsN. Highlighted are the GaAsN and GaInAs ternaries, as well as the lattice-matched GaInAsN quaternary.

- **Lower system supply voltage:** Because of the reduced turn-on voltage, circuits utilizing GaInAsN HBTs will require a lower overall system voltage. The lower system voltage enables GaAs-based power amplifier circuits to operate with the smaller batteries needed for future commercial wireless communication systems. The lower turn-on voltage will also enable better functionality in digital circuits which are currently constrained by the standard power supplies used for Si circuits. Note that this reduction in voltage eliminates one of the principal advantages of InP-based HBTs over GaAs-based HBTs [7].

- **Improved temperature stability:** The increase in collector current density associated with the reduction in turn-on voltage increases the neutral base recombination component of the base current relative to the reverse hole injection component, and thus improves the temperature stability of the peak DC current gain.

- **Better RF performance:** GaInAsN alloys enable the implementation of several device structures, such as a graded energy-gap base, which enhance RF performance.

- **Increased reliability:** The reliability of GaInAsN HBTs may be improved over conventional GaAs HBTs due to the increased robustness of material with In and N doping (alloy hardening), increased hole confinement, and suppressed $n=2$ base current components. We are currently working on a model which qualitatively accounts for the general reliability trends reported in the literature. If correct, the lower turn-on voltage itself may improve reliability by reducing the hole injection component of the base current for a fixed collector current density [8].

- **Higher low bias DC current gain:** An increase in the collector current relative to fixed $n=2$ base current components leads to a higher DC current gain at low bias and a more stable gain as a function of current density.
- **Increased circuit design flexibility:** In addition to relaxing the constraints on power supply voltage, the lower turn-on voltage and stable gain as a function of both voltage and temperature gives circuit designers more latitude to optimize amplifier circuit parameters such as linearity and power add efficiency (PAE). A lower turn-on voltage implies that a given current can be achieved at lower bias, allowing a higher PAE to be achieved at low applied bias. Linearity may also be improved by a resulting increase in the reverse bias on the base-collector junction. In digital circuits, a lower bias voltage should reduce the power-delay products [1].
- **Reduced process sensitivity:** The impact of $n=2$ recombination processes at the emitter-base junction and the emitter periphery will be reduced due to the increased collector current. Thus GaInAsN HBTs may not require passivating ledges, reducing processing complexity and cost.

During our Phase I effort, we have demonstrated a 10 to 15 meV reduction in the turn-on voltage of GaAs-based HBTs. We have also proven the feasibility of increasing the level of N, C, and In incorporation in p-type GaAs films, which should lead to further reductions in the turn-on voltage during the Phase II effort. These accomplishments are described in the following sections. We also outline the technical challenges that may be encountered during the Phase II program, and give a brief description of the Yale effort to explore the growth of GaAsN alloys over the full compositional range (N-doped GaAs to As-doped GaN).

InGaP/GaInAsN HBTs with Reduced Turn-on Voltage

The current-voltage characteristics of an HBT are often characterized by reference to a turn-on voltage defined as the base-emitter voltage (V_{be}) required to achieve a certain fixed collector current (I_c) [1]. While in theory V_{be} is a function of base layer properties only (Equation 1), in practice emitter properties often increase V_{be} from its theoretical value. Discontinuities in the energy-band line-up at the base-emitter heterojunction in an HBT can cause a spike in the conduction band which limits the collector current and hence raises V_{be} . As a result, GaAs-based HBTs in general, and AlGaAs/GaAs HBTs in particular, can vary tremendously in their turn-on voltage depending on how the base-emitter interface is grown [9-10]. However, if this conduction band is properly controlled, the turn-on voltage of GaAs-based HBTs can approach the theoretical lower limit of diffusion-limited current flow across a pn junction. As given in Equation 1, the turn-on voltage on an HBT is then fundamentally limited by the energy-gap of the base layer. We believe that the InGaP/GaAs HBTs grown at Kopin routinely exhibit this fundamental lower limit in turn-on voltage set by the energy-gap of GaAs. During this Phase I effort, we have demonstrated InGaP/GaInAsN HBTs with turn-on voltages 10-15 meV below the level of standard InGaP/GaAs HBTs. These lower turn-on voltages result from a decrease in the energy-gap of the base layer due to the incorporation of In and N. To confirm the properties of the base layer, secondary ion spectrometry (SIMS), photoluminescence (PL), double crystal x-ray diffraction (DCXRD), and Polaron C-V profiling measurements have been performed on an InGaP/GaInAsN HBT with a 1500 Å thick base.

Equation 1 describes the turn-on voltage of a p⁺n junction assuming the collector current is governed by the Shockley equation. By rewriting the product of base doping and thickness in terms of the base sheet resistance (R_s base), the turn-on voltage (V_{be}) can be expressed as a function of base sheet resistance:

$$V_{be} = -B \ln[R_s \text{base}] + A,$$

where

$$A = E_{gb}/q - (kT/q) \ln[q^2 \mu N_c N_v D_n / J_c]$$

and

$$B = (kT/q).$$

Figure 2 shows the turn-on voltage, as derived from large area devices (emitter dimensions 75 μm x 75 μm) at a current of 1E-4 A ($J_c = 1.78 \text{ A/cm}^2$), for a large number of InGaP/GaAs HBTs grown at Kopin. The V_{be} of the InGaP HBTs qualitatively follows the natural logarithm dependence on R_s base described above. There is no evidence that a conduction band spike limits the collector current of standard InGaP/GaAs HBTs grown at Kopin. The collector current ideality factor is nearly one on all InGaP/GaAs HBTs, and examination of the reverse Gummel plots from these devices shows no indication of a conduction band spike limiting the collector current [10]. To further confirm the nature of the collector current in Kopin's InGaP/GaAs HBTs, we grew a series GaAs emitter/GaAs base BJT structures with varying base thickness. The V_{be} from these structures,

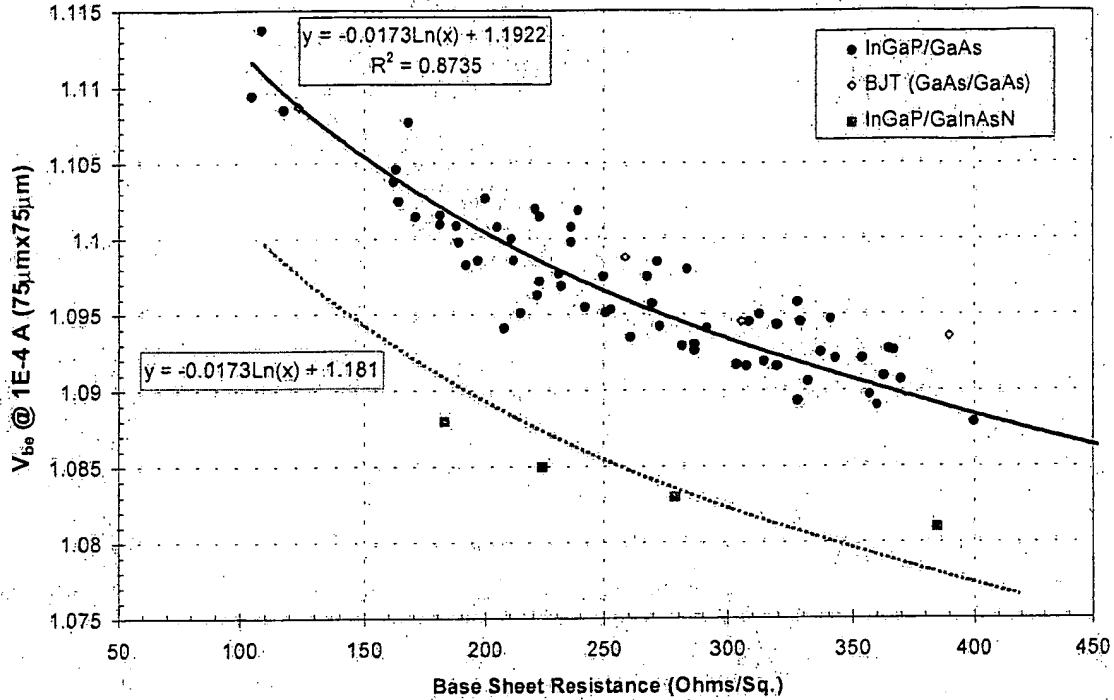


Figure 2: Turn-on voltage ($V_{be}@1.78A/cm^2$) as a function of base sheet resistance for standard InGaP/GaAs HBTs, GaAs/GaAs BJTs, and InGaP/GaInAsN HBTs. The solid line represents a logarithmic fit to the InGaP/GaAs HBT data, the dashed line a 11.2 meV reduction to the fitted data as a guide to the eye for the InGaP/GaInAsN data.

which clearly do not have any conduction band spike, follows the same logarithmic dependence as Kopin's InGaP/GaAs HBTs (Figure 2). Thus the InGaP/GaAs turn-on voltage data in Figure 2 represents the lower limit of V_{be} which can be achieved using a GaAs base layer, and can become a metric for gauging the success of lowering the turn-on voltage by using a lower energy-gap GaInAsN base.

During this Phase I STTR program, we grew a series of InGaP/GaInAsN HBTs with varying base thickness resulting in R_s base values between 183 and 385 Ω/\square . The basic device structure used to explore the impact of In- and N-doping on GaAs HBTs is shown in Figure 3. The structure consists of a GaAs buffer layer, Si-doped GaAs subcollector and collector layers, C-doped GaInAsN base layer with thickness varying between 700 and 1500 Å, a wide band gap InGaP emitter, and GaAs and InGaAs emitter contact layers. These structures were processed into large area devices using Kopin's standard QL process; the turn-on voltage, Gummel plots, and dc current gain from the resulting devices are shown in Figures 2, 4, and 5, respectively. As a guide to the eye, the dashed line in Figure 2 shows an 11.2 meV shift downward in the V_{be} relative to InGaP/GaAs HBTs. The magnitude of the V_{be} shift seen in the InGaP/GaInAsN HBTs appears to decrease with increasing base sheet resistance. This is likely a real phenomenon related to non-uniform In incorporation across the width of the base layer. However, the V_{be} of all four GaInAsN base structures is clearly below that observed in HBTs with GaAs base layers. The DC current gain, while not high, is greater than 10 in all three InGaP/GaInAsN structures over

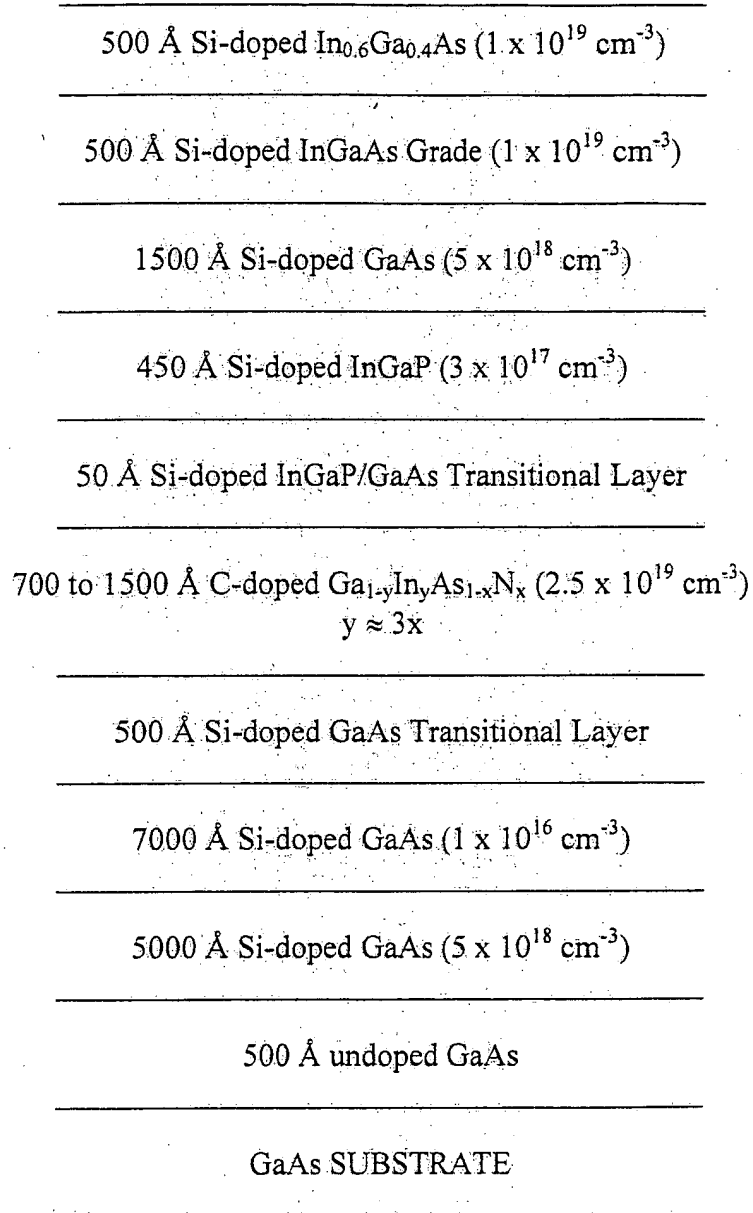


Figure 3: Schematic of a GaAs-based HBT using a nearly lattice-matched GaInAsN base.

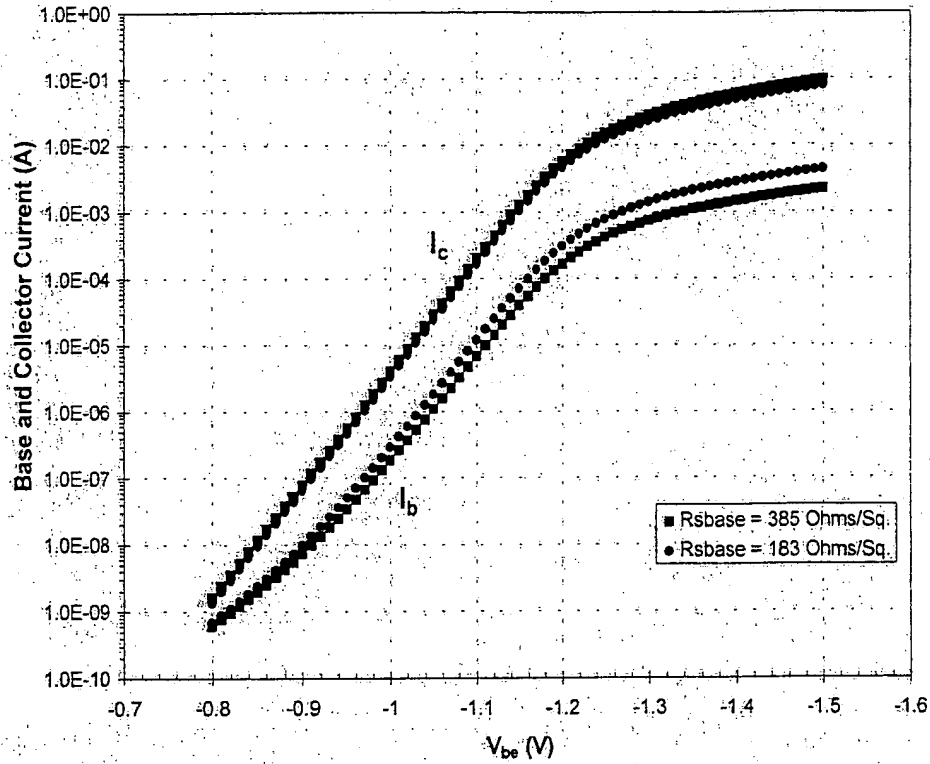


Figure 4: Gummel plots from InGaP/GaInAsN structures with base sheet resistance values of 183 and 385 Ω/\square . Emitter mesa dimensions are 75 μm x 75 μm .

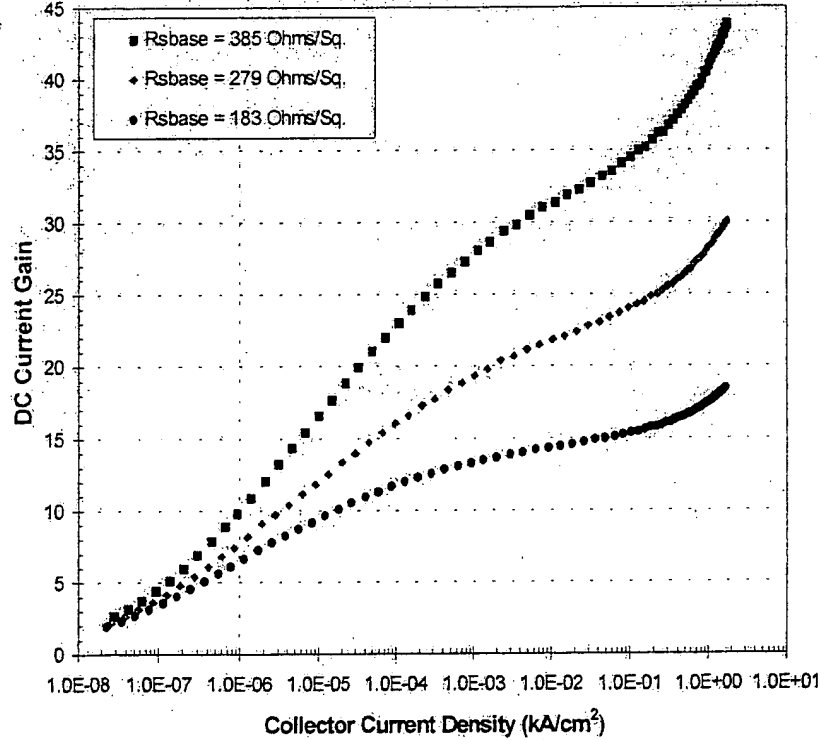


Figure 5: DC current gain as a function of collector current density for the GaAs/GaInAsN HBTs with varying base width, and hence varying base sheet resistance ($R_{s\text{base}}$).

five decades of current (Figure 5). As is typical for InGaP/GaAs HBTs, the base and collector currents do not cross over the bias range measured (Figure 4).

SIMS profiles through the thickest base structure indicate the In composition is close to 4% and the N concentration is on the order of $1\text{E}18\text{ cm}^{-3}$ in the base layers of these GaInAsN HBTs (Figure 6). The C level is over $2\text{E}19\text{ cm}^{-3}$ and the H level is below $4\text{E}18\text{ cm}^{-3}$. The C, H, N, and In levels are not constant through the base layer, but exhibit a small oscillation near the base-collector interface. This oscillation in dopant impurities also manifests itself electrically as an oscillation in carrier concentration, as seen in the Polaron profile in Figure 7. The average carrier concentration in the base layer of the InGaP/GaInAsN HBTs is $2.6\text{E}19\text{ cm}^{-3}$ as measured by Polaron. This value is in rough agreement with Hall measurements made on bulk calibration samples.

The base layer is of sufficient thickness on the $183\ \Omega/\square$ structure to allow DCXRD and PL measurements on the full HBT structure. Figure 8 shows the DCRXD spectrum from the InGaP/GaInAsN HBT and a standard InGaP/GaAs HBT of comparable base thickness. In the standard sample, the $4\text{E}19\text{ cm}^{-3}$ base layer is seen as a shoulder on the right hand side of the substrate peak, approximately corresponding to a position of $+90$ arcsecs. With the addition of In, the base layer peak is pushed to -425 arcsec on the InGaP/GaInAsN structure. The PL spectrum from both the InGaP/GaAs and InGaP/GaInAsN structures are shown in Figure 10. Liquid N₂ PL measurements were taken after etching off the InGaAs and GaAs cap layers, selectively stopping at the top of the InGaP emitter. In both structures the strongest emission is from the GaAs collector layer at 8228 Å (1.507 eV). However, emission from the base layer is also clearly visible in both structures. Band filling due to the high carrier concentration leads to a broad emission around 1.459 eV in the standard InGaP/GaAs structure. The energy of the base layer emission has been pushed out 64 meV to 1.395 eV in the InGaP/GaInAsN HBT. We have not yet determined why only part of this 64 meV reduction in peak PL emission has been manifested as a reduction in V_{be} .

The electrical properties of the InGaP/GaInAsN HBT have also been compared to a standard InGaP/GaAs structure. Figure 10 compares the Gummel plots of two InGaP emitter structures with comparable base sheet resistance values (183 and $174\ \Omega/\square$) but different base layer materials. The device with the GaInAsN base layer shows a clear shift upwards in collector current (by a factor of 1.9) compared to the conventional GaAs base structure, and has an identical collector current ideality factor of 1.01. However, the base current of the GaInAsN base structure is also higher at all bias levels, resulting in a lower DC current gain (Figure 11). During the Phase II effort we will need to focus on improving the minority carrier lifetime of the InGaAsN base layer as well as the emitter layer grown on top of the N-containing base.

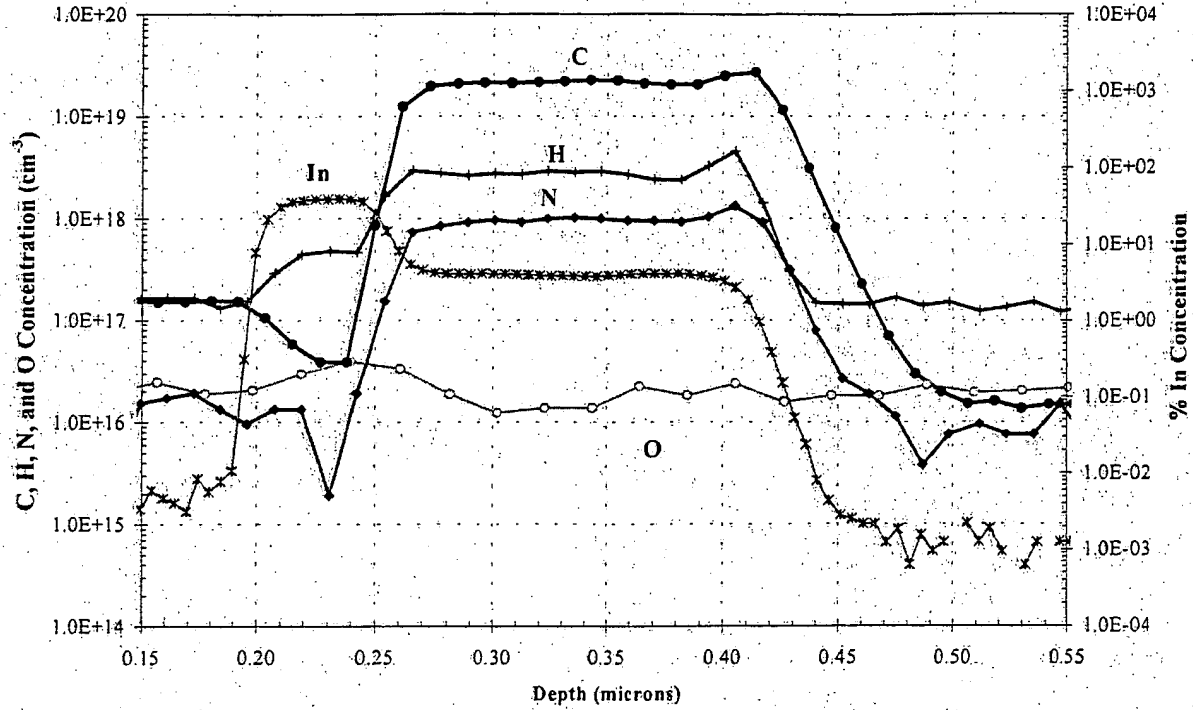


Figure 6: SIMS profiles of the C, H, N, O, and In concentrations in the base layer of the 183 Ω/\square InGaP/GaInAsN HBT structure.

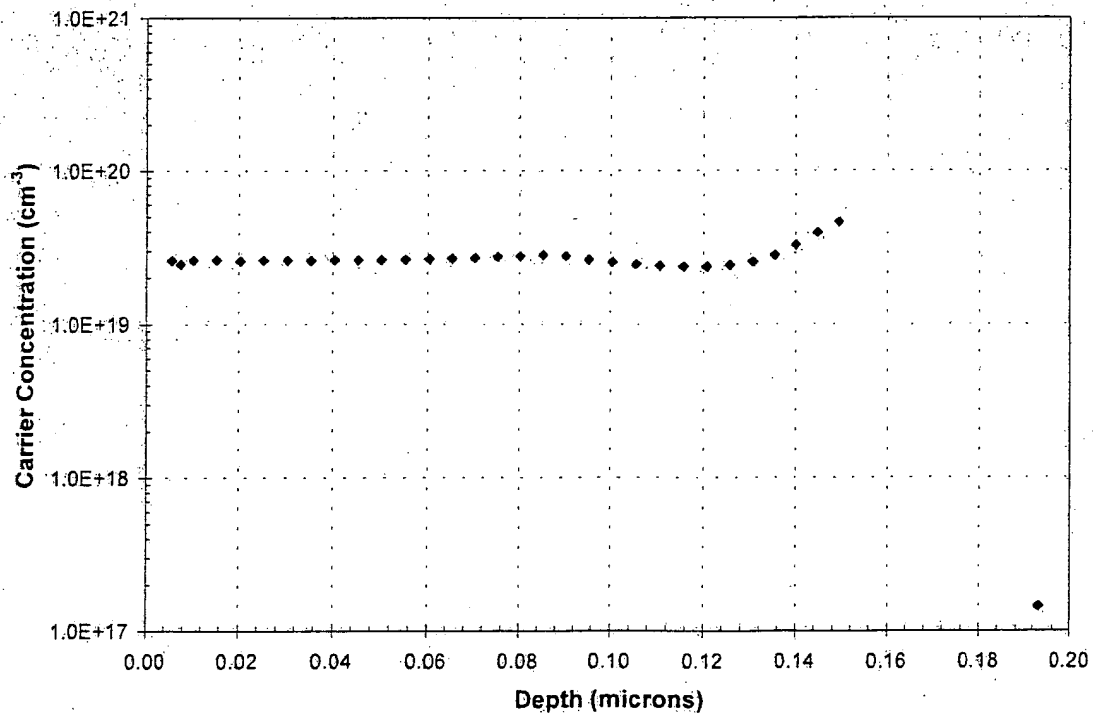


Figure 7: Polaron C-V p-type doping profile through the base layer of the 183 Ω/\square InGaP/GaInAsN structure.

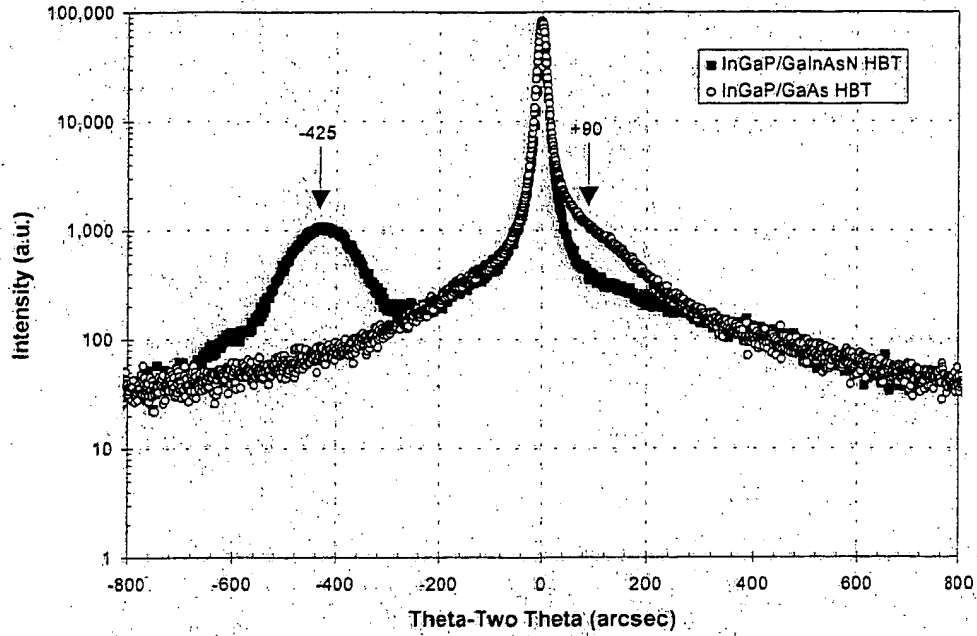


Figure 8: DCXRD spectrums from a standard InGaP/GaAs HBT and the InGaP/GaInAsN structure, both with a nominal base thickness of 1500 Å. The position of the base layer peaks are marked.

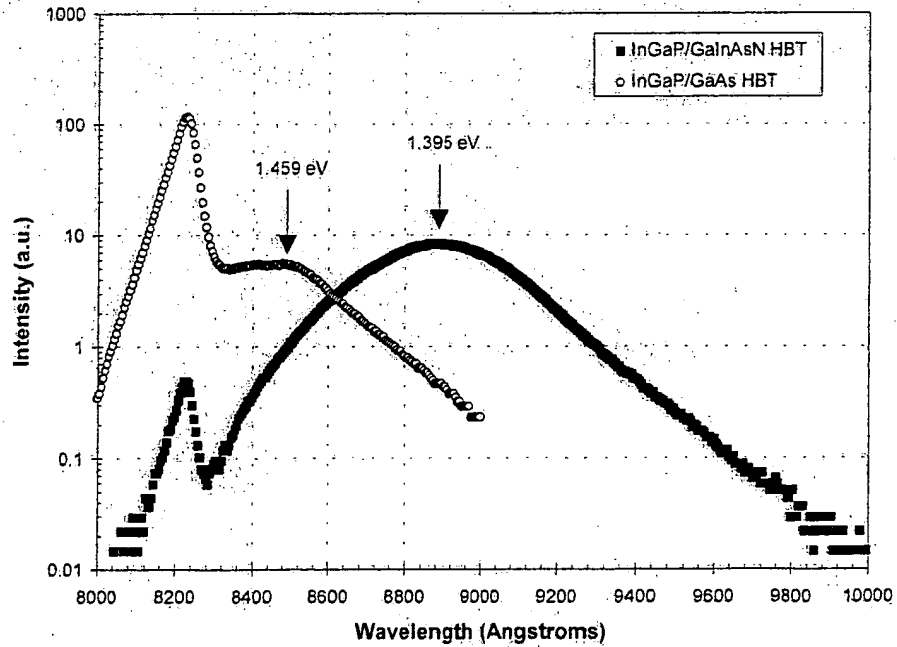


Figure 9: Liquid N₂ PL spectrums from a standard InGaP/GaAs HBT and the InGaP/GaInAsN structure, both with a nominal base thickness of 1500 Å. PL spectrums were taken after etching down to the InGaP emitter. The position of the base layer peaks are marked.

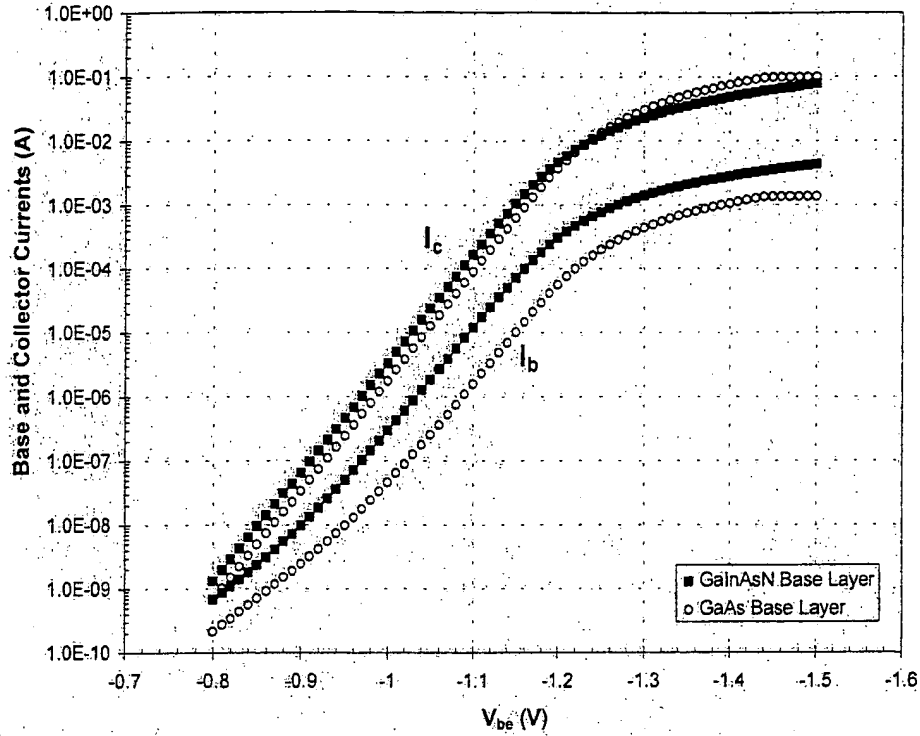


Figure 10: Gummel plots from InGaP/GaInAsN and InGaP/GaAs HBT structures ($75\ \mu\text{m} \times 75\ \mu\text{m}$) with comparable base sheet resistance values of 183 and $174\ \Omega/\square$.

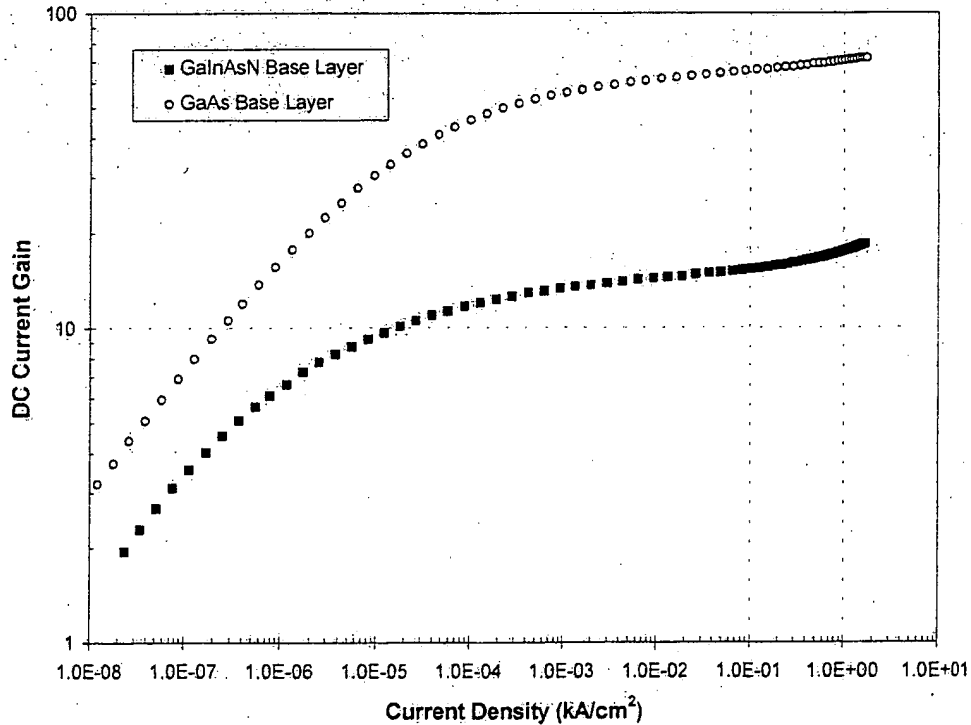


Figure 11: DC current gain as a function of collector current density from the InGaP/GaInAsN and InGaP/GaAs HBT devices in Figure 10.

Incorporation of N, In, and C in GaAs

The large area device results obtained from InGaP/GaInAsN HBTs, which were discussed in the previous section, clearly suggest the feasibility of lowering the turn-on voltage of GaAs-based HBTs by adding In and N to the base layer. However, to push the device performance to a higher level, we need to increase the C, N, and In concentrations of the GaInAsN base layer material while at the same time improving the minority carrier lifetime. During our Phase I effort, we have made significant progress towards this goal, incorporating over $1 \times 10^{19} \text{ cm}^{-3}$ of N, $1 \times 10^{20} \text{ cm}^{-3}$ of C, and 4% In into p-type GaAs. The resulting material exhibits significant shifts in both the energy-gap and lattice constant as measured by photoluminescence and DCXRD. In this section, we report on our Phase I progress at incorporating N, In, and C into GaAs both separately and simultaneously. The growth chemistry is clearly complex and interactive, leading to everything from changes in growth rate to memory effects impacting the growth of overlying material. Understanding and manipulating these interactive effects will be one of the key technical challenges of the Phase II effort.

During the Phase I program, we have determined that NH_3 is a suitable source for growing N-doped GaAs films, even at low temperatures. The SIMS profile of the N concentration in a $2 \mu\text{m}$ p-type GaAs film containing five layers with different N source flows is shown in Figure 12. The peak N concentration is $8.4 \times 10^{18} \text{ cm}^{-3}$. The O and Si levels in this sample are below the detection level, while the C concentration ranges from 3.5 to $6.9 \times 10^{19} \text{ cm}^{-3}$. Most encouraging is the plot of N concentration versus N source flow shown in Figure 13. A least squares fit indicates the N concentration is increasing linearly with N source flow and suggests that increasing the N concentration in the films is simply a matter of increasing the source flow for any given set of growth conditions. The N incorporation has also been found to be a function of growth temperature and gas-phase V/III ratio.

The addition of In to GaAsN can be used to both further lower the energy-gap and adjust the lattice constant. When doping with carbon, the lattice constant of GaAs shrinks, causing the film peak in a double-crystal x-ray diffraction (DCXRD) spectrum to shift to the right of the GaAs substrate. For C-doping levels near the $4 \times 10^{19} \text{ cm}^{-3}$, the film DCXRD splitting is typically around $+90$ arcsec. Adding N shifts the peak film further to the right and thus increases the splitting. However, when In is added, the lattice constant expands, pushing the film peak to the left. Figure 14 shows the DCXRD spectrum from four GaInAsN samples with different levels of In source flow added to the growth. The film peak splitting moves from approximately $+445$ arcsec with no In flow to -572 arcsec with the highest In flow in these bulk samples. Growth temperature has also been found to have a strong impact of In incorporation. The 64 meV shift in PL emission seen in the HBT structures from Figure 9 is comparable to that seen in bulk GaInAsN samples.

Carbon is the dopant of choice in modern GaAs-based HBTs because of its low diffusivity. Any potential advantages of using GaInAsN alloys for HBTs must be accomplished in films which are co-doped with C. Growth chemistry, however, can play a role in hindering C incorporation in GaAs-based alloys. Historically, it has been very difficult to grow carbon doped GaInAs using TMIIn. At the onset of the Phase I effort, concerns of diminished C incorporation discouraged us from adding In to GaAsN. However, experiments conducted part way through the Phase I effort

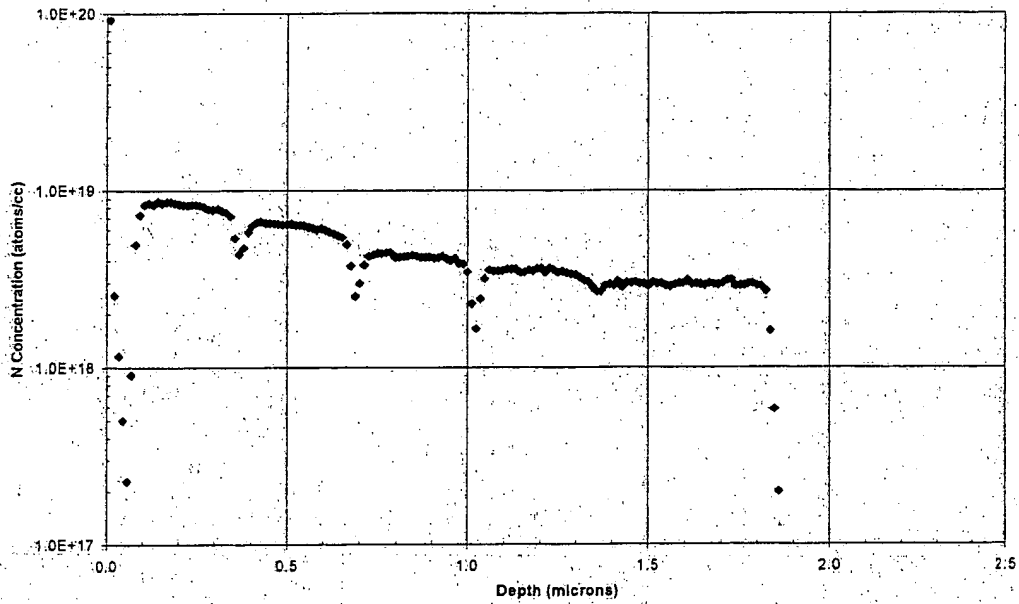


Figure 12: SIMS profile of the N concentration through a p-type GaAs sample consisting of five layers with different N source flows.

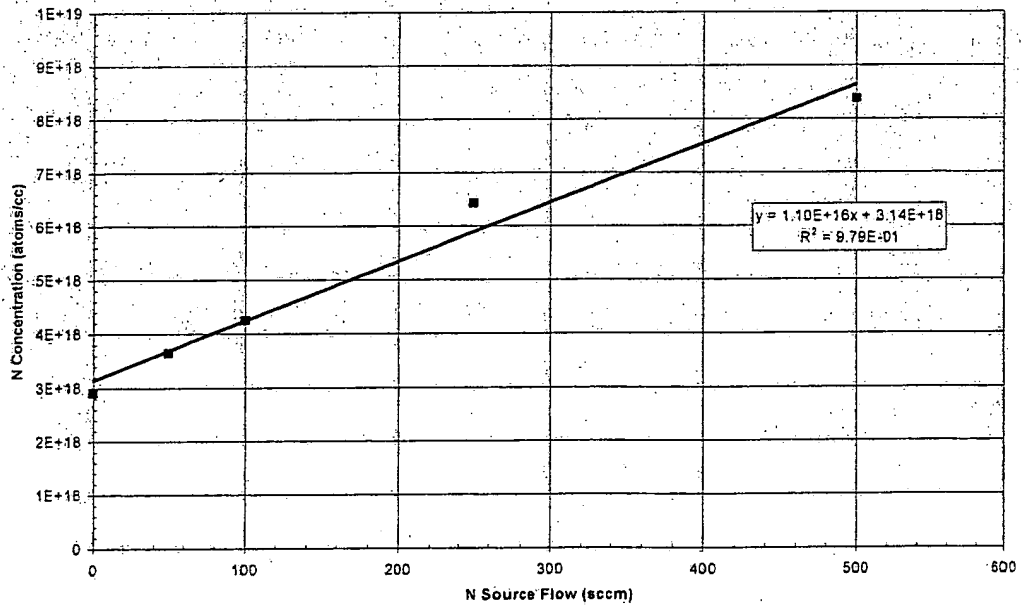


Figure 13: Average N concentration in the five layers shown in Figure 4 as a function of N source flow. The solid line represents a least squares linear fit of the data.

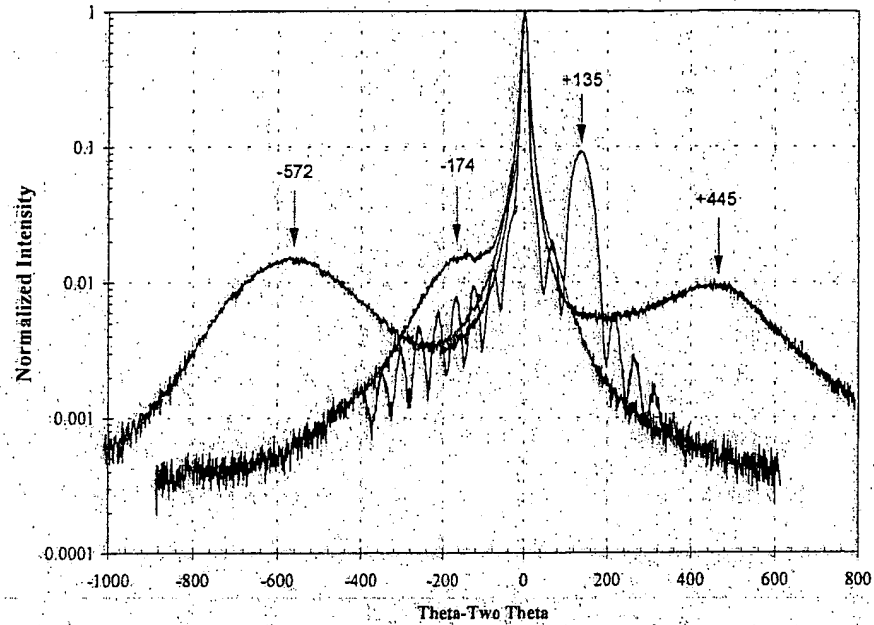


Figure 14: DCXRD of bulk (5000 Å) GaInAsN layers grown with varying In, N, and C source flows. As the In source flow increases, the film peak shifts to the left (arrows).

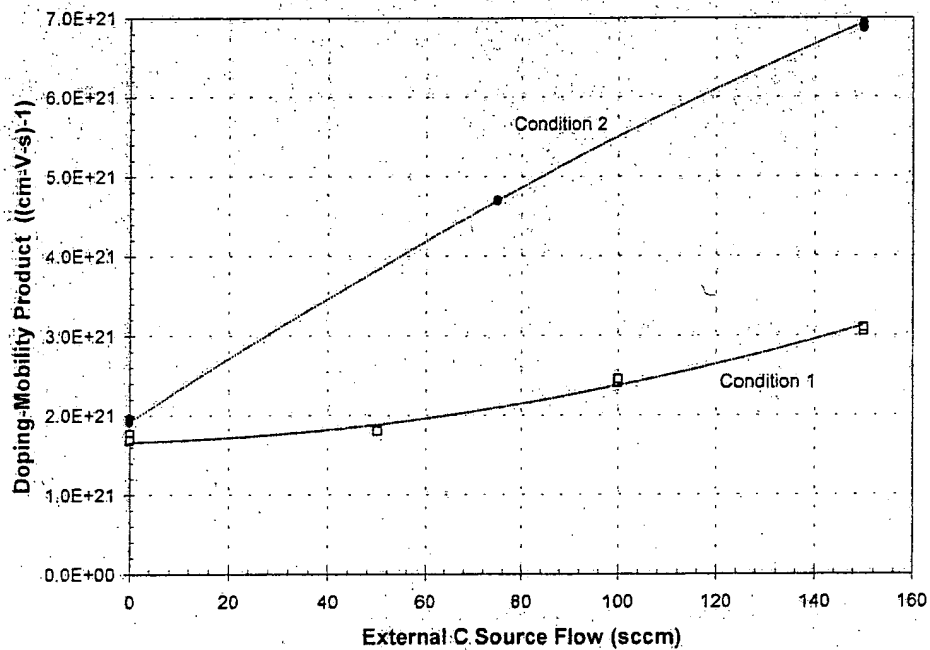


Figure 15: Doping-mobility product in bulk p-type GaInAs bulk layers as a function of external carbon source flow. The product is determined from measurements of sheet resistance and thickness.

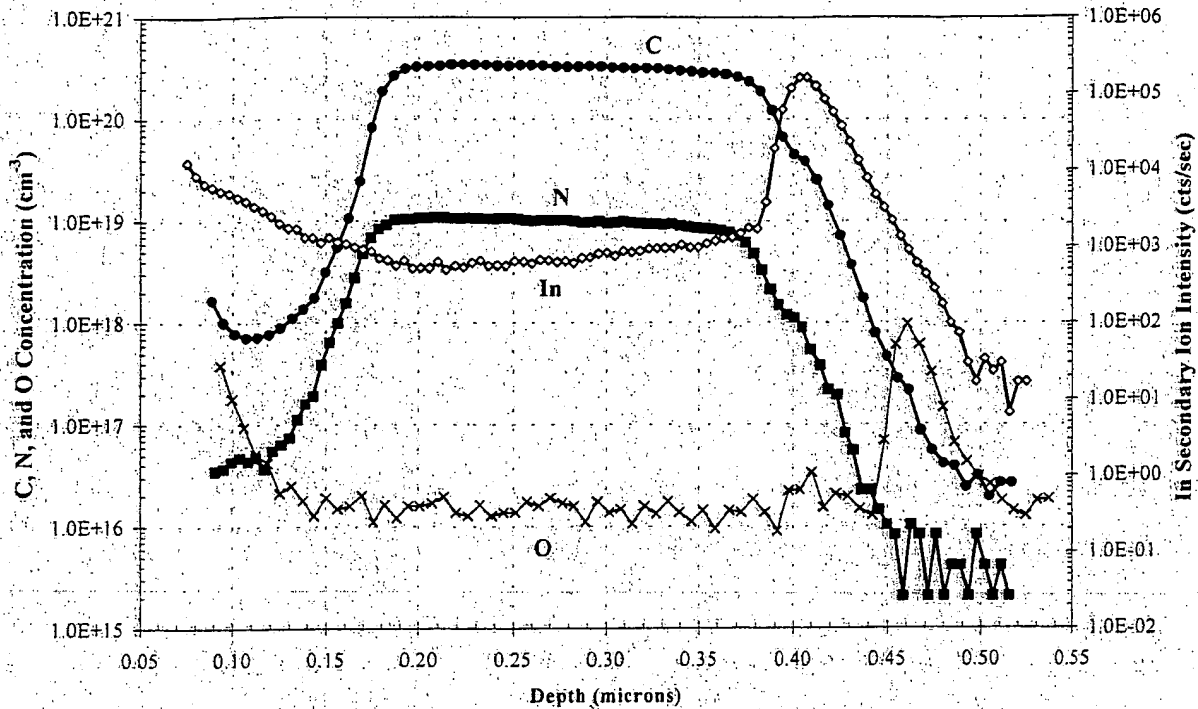


Figure 16: SIMS of a thick (~ 5000 Å) p-type GaAs sample co-doped with In and N.

suggested that growth conditions have a strong impact on C and In incorporation, and under some conditions it is possible to add significant quantities of both C and In. SIMS analysis of some In-containing samples indicate the C levels are well above $4E19 \text{ cm}^{-3}$. Electrical measurements indicate that under optimized growth conditions it is possible to maintain both high C concentration and a high percentage of electrical activation of the C in InGaAs. Figure 15 shows the impact of an external C source flow on the doping-mobility product of p-type InGaAs films grown under two different sets of conditions. The doping-mobility product is used as the metric because it removes the uncertainty associated with mobility measurements in heavily doped p-type layers. We expect a film with $4E19 \text{ cm}^{-3}$ p-type doping and a mobility of $90 \text{ cm}^2/\text{V-s}$ to have a doping-mobility product of $3.6E21 (\text{V-cm-s})^{-1}$. The mobility is expected to decrease as the doping level increases, making the mobility-doping product less sensitive to changes in doping. Under growth Condition 2, then, we have achieved doping levels that are probably in excess of $8E19 \text{ cm}^{-3}$.

In addition to experiments exploring the incorporation of N in GaAs, In in GaAsN, and C in GaInAs, we have grown layers simultaneously incorporating N, In, and C. Figure 16 shows the SIMS profile through a bulk p-type GaInAsN structure with a C level over $3.2E20 \text{ cm}^{-3}$, N level over $1E19 \text{ cm}^{-3}$, and an unquantified In level two orders of magnitude above background levels. While the level of C, In, and N incorporation in this sample is encouraging, the minority carrier properties need to be improved. PL emission from this sample is extremely weak, and the H level is very high ($>1E20 \text{ cm}^{-3}$).

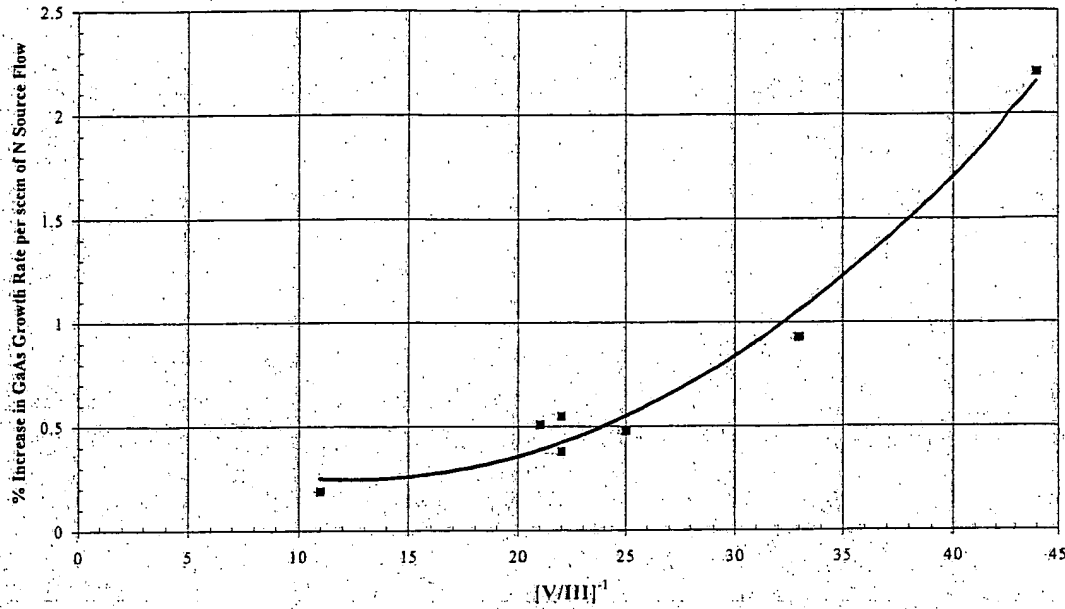


Figure 17: Effect of nitrogen source flow on GaAs growth rate as a function of arsenic and gallium source flows. The V/III gas flow ratio has been varied by changing both the gallium and arsenic source flows. The impact of N source flow on GaAs growth rate has been assumed to be linear.

While we have been successful at growing GaInAsN films with large C concentrations, the growth mechanisms behind N-containing, C-doped InGaAs-based films are not well understood. The initial Phase I studies suggest that growth temperature, source flows, and growth chemistry all play important roles in N, C, and In incorporation. Initial results also indicate a complex growth chemistry with many interactive effects between the growth parameters. For example, at low nitrogen source flows, the GaAs growth rate increases with increasing nitrogen source flow. Moreover, the magnitude of this effect of nitrogen source flow on GaAs growth rate varies dramatically with the gallium and arsenic source flows. Figure 17 shows the percent increase in growth rate per sccm of nitrogen source flow as a function of inverse V/III gas flow ratio. A set of single layer, bulk (5000 Å) structures were grown and characterized by Hall, selective etch, DCXRD, and PL. Under some conditions, a 50 sccm nitrogen source flow can lead to over a 50% increase in the GaAs growth rate. These results suggest that the nitrogen source flow acts as a catalyst for the decomposition of gallium and arsenic sources. Since most models of the MOCVD growth of GaAs hypothesize that gallium and arsenic source molecules interact on the surface, the results summarized in Figure 17 suggest the nitrogen source may interact with both the gallium and arsenic source molecules on the growth surface and not in the gas stream.

During our Phase I effort, we have seen evidence which suggests that N may be incorporated into the emitter layer grown above a N-containing base layer. At this point, the exact nature of this unwanted N (or other contaminant) is unclear, but it is likely due to residual source gas which is not swept out of the growth chamber. Figure 18 compares the Gummel plots of an InGaP/GaInAsN HBT to a standard GaAs-based HBT. The GaInAsN in the base layer of this HBT contains higher levels of N and C than is present in the devices discussed in the previous

section (Figures 4 and 5). The InGaP/GaInAsN HBT exhibits two serious problems: an increase of nearly five orders of magnitude in the base current at low bias, and a very large effective series resistance. Previously, we have used a basic device model to analyze the Gummel plots of large area devices in which surface recombination mechanisms can be ignored [9,11]. In this device model, the collector current is fit by a simple diode equation, and the base current is the sum of the three components: space charge recombination, neutral base recombination, and reverse hole injection. For a given emitter structure, the magnitude of the space charge recombination component can be related to the trap density in the emitter. Analysis of the Gummel plots in Figure 18 indicate the trap density in the InGaP emitter grown on top of the GaInAsN is orders of magnitude higher than the trap density in InGaP grown on top of standard p-type GaAs. On the other hand, Figure 19 compares the Gummel plots of GaAs emitter structures. In this case, the trap density of the GaAs emitter appears identical when grown on either GaInAsN or standard p-type GaAs. However, the effective series resistance remains quite large on the GaInAsN base sample, leading to the quick roll-over of the collector and base currents. Resolving these base current and series resistance problems is a key technical challenge for the Phase II effort.

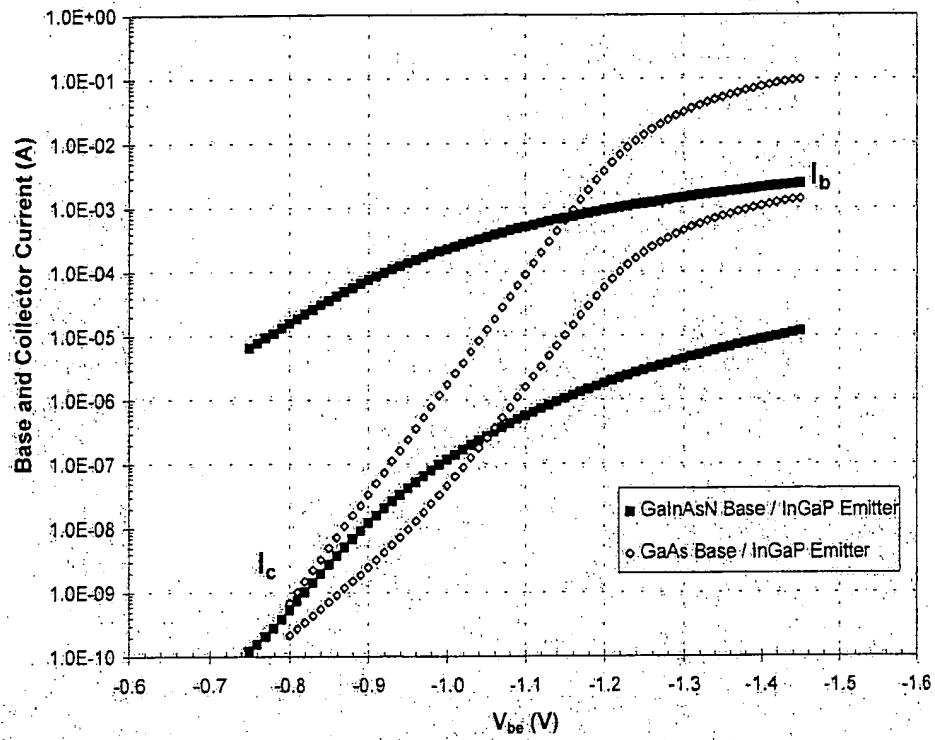


Figure 18: Gummel plots from GaInAsN and GaAs base layer structures with an InGaP emitter.

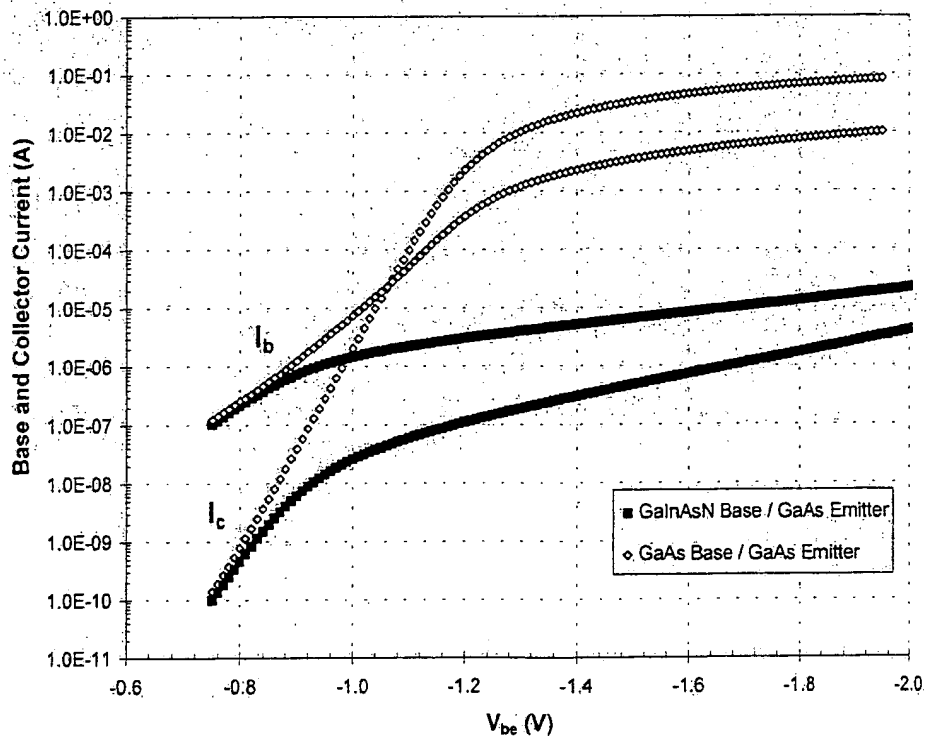
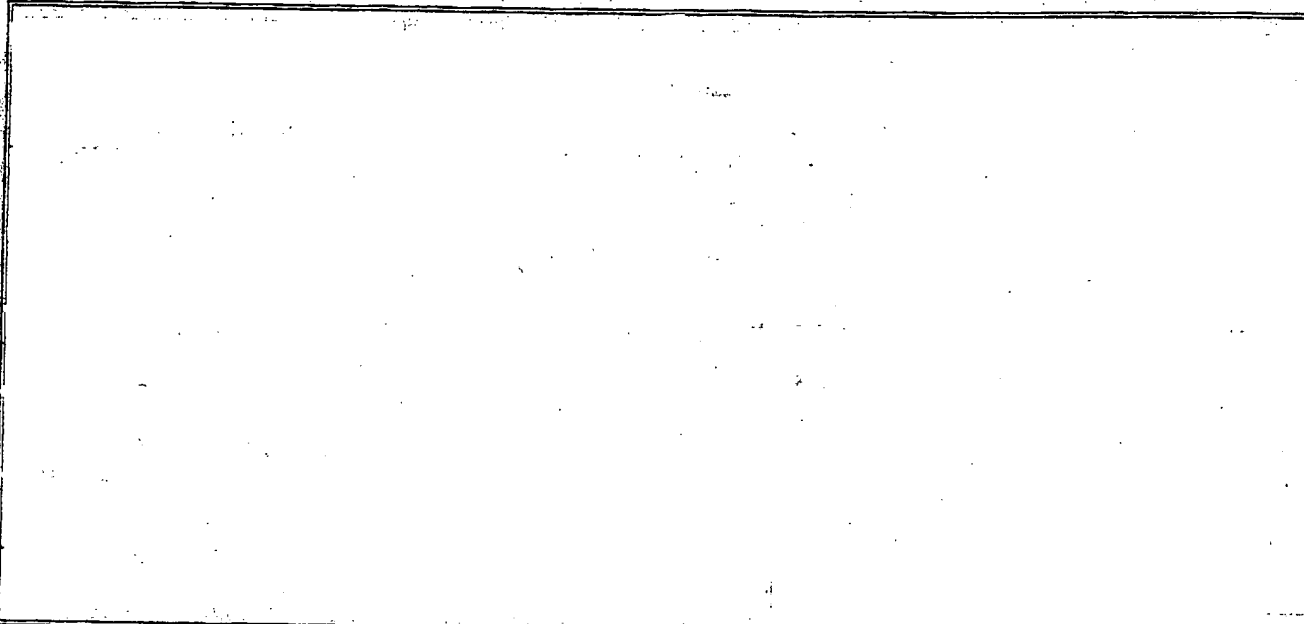


Figure 19: Gummel plots from GaInAsN and GaAs base layer structures with a GaAs emitter.

TOPIC NUMBER:	PROPOSAL TITLE: Low-Voltage GaAs-Based HBTs	
PRINCIPAL INVESTIGATOR: Roger E. Welser	PI TELEPHONE:	
PROPOSED COST:	PHASE I OR II: Phase II	PROPOSED DURATION IN MONTHS: 24



YES ☒ NO ☐

☒☐ ☒☐ ☒

144

☐ ☒

For any purpose other than to evaluate the proposal, this data except Appendix A and B shall not be disclosed outside the Government and shall not be duplicated, used or disclosed in whole or in part, provided that if a contract is awarded to this proposer as a result of or in connection with the submission of this data, the Government shall have the right to duplicate, use or disclose the data to the extent provided in the funding agreement. This restriction does not limit the Government's right to use information contained in the data if it is obtained from another source without restriction. The data subject to this restriction is contained on the pages of the proposal listed on the line below.

**U.S. DEPARTMENT OF DEFENSE
SMALL BUSINESS TECHNOLOGY TRANSFER (STTR) PROGRAM
PROPOSAL COVER SHEET**

Failure to fill in all appropriate spaces may cause your proposal to be disqualified

TOPIC NUMBER:		PROPOSAL TITLE: Low-Voltage GaAs-Based HBTs									
PHASE I OR II PROPOSAL: Phase II		FIRM NAME: Kopin Corporation	PRINCIPAL INVESTIGATOR: Roger E. Welser								
<p>TECHNICAL ABSTRACT (Limit your abstract to 200 words with no classified or proprietary information/data)</p> <p>Kopin intends to work closely with both university and industrial partners during this Phase II project to develop and commercialize low-voltage GaAs-based heterojunction bipolar transistors (HBTs) for high frequency microwave and millimeterwave applications. Low voltage operation within a GaAs platform is enabled by an exciting new material system, GaInAsN. Numerous laboratories have demonstrated that the energy-gap of GaInAs drops substantially when small amounts of N are incorporated into the material. Moreover, because N pushes the lattice constant in the opposite direction from In, GaInAsN alloys can be grown lattice-matched to GaAs and thus eliminate the problems associated with strain. During our Phase I effort, we developed a proprietary growth process for synthesizing heavily p-type GaInAsN, which, unlike all other reported processes, is entirely compatible with high volume manufacturing. The potential benefits of an HBT structure incorporating GaInAsN in the base include lower turn-on voltage, stable current gain, improved high frequency performance, and increased long term reliability. This integrated Phase II effort will range from basic material studies to device fabrication and reliability testing and will lay the groundwork for the commercialization of future generations of high frequency microwave circuits.</p>											
<p>ANTICIPATED BENEFITS/POTENTIAL COMMERCIAL APPLICATIONS OF THE RESEARCH OR DEVELOPMENT</p> <p>The proposed technology is intended to lead to the realization of high-performance, low-cost HBTs for dual-use high frequency microwave applications. HBTs are playing an increasing role in commercial wireless communication systems and in a variety of both ground- and space-based military applications. If successful, this program will lead to microwave components combining the advantages and the maturity of GaAs-based technology with the low turn-on voltages of InP- and SiGe-based devices. Such components are crucial for achieving communication systems operating with low voltage power supplies.</p>											
<p>KEYWORDS (List a maximum of 8 Keywords that describe the project)</p> <table> <tr> <td>Heterojunction Bipolar Transistor</td> <td>GaAsN</td> </tr> <tr> <td>GaAs HBT</td> <td>MOCVD</td> </tr> <tr> <td>Microwave Communication</td> <td>Strained-Layer Epitaxy</td> </tr> <tr> <td>X-band High Power Amplifier</td> <td>Reliability</td> </tr> </table>				Heterojunction Bipolar Transistor	GaAsN	GaAs HBT	MOCVD	Microwave Communication	Strained-Layer Epitaxy	X-band High Power Amplifier	Reliability
Heterojunction Bipolar Transistor	GaAsN										
GaAs HBT	MOCVD										
Microwave Communication	Strained-Layer Epitaxy										
X-band High Power Amplifier	Reliability										

Identification and Significance of the Problem

GaAs-based HBTs are gaining wide acceptance as critical components in a wide range of circuits required for both wireless and wired communication systems. As a leading producer of GaAs-based HBT wafers by the metalorganic chemical vapor deposition (MOCVD) technique, Kopin Corporation has played an important role in developing the materials necessary for reliable, high performance devices. However, future trends in the commercial wireless communications market are expected to require lower voltage operation, higher frequency performance, and lower cost production. Military applications can also benefit from these attributes. In addition, military systems, such as phased array radar systems, high speed A/D converters, electronic countermeasures, and satellite communications, require high power semiconductor amplifiers operating at the X-band and beyond (>10 GHz). While GaAs-based HBTs currently meet some of these needs, higher frequency performance and longer device reliability are necessary to meet future needs. Moreover, these device improvements need to be met while lowering the overall system voltage in both ground- and space-based applications. Thus there are incentives in both the commercial and military markets to find novel approaches for improving the performance and lowering the cost of GaAs-based HBTs.

The increasing trend toward lower supply voltages in many communication systems has spurred a great interest in material systems enabling HBTs with low turn-on voltages, high power added efficiency, high linearity, and high output powers. Although InP-based HBTs offer low turn-on voltages with respectable power performance, the process and growth technology needs substantial work to reach volume production. The difficulty of C-doping InGaAs lattice-matched to InP and the unavailability of large area substrates for manufacturing also limit the potential of InP-based HBTs. At the laboratory level, SiGe-based HBTs have demonstrated reasonable RF performance and low turn on-voltages, but good power handling capabilities, long-term reliability, and volume manufacturability still need to be proven. The potential payoff would be tremendous if GaAs-based HBTs can be engineered to realize low turn-on voltages.

If the proper steps are taken to minimize the conduction band spike at the emitter-base junction, the turn-on voltage of an HBT is limited by the energy-gap of the base layer [10]. It is well-known that the addition of In to GaAs lowers the energy-gap. However, GaInAs alloys have a larger lattice constant and thus produce undesirable strain when incorporated within a GaAs-based device structure. Recently, there have been numerous reports concerning GaAs and related compounds doped with small amounts of N [1-3]. Such GaAsN alloys have a number of interesting properties, not the least of which is a very large reduction in energy gap with the addition of small amounts of N. Moreover, the lattice constant of GaAs shrinks rather than expands with the addition of N. By adding both In and N to GaAs, it is possible to dramatically lower the energy-gap while maintaining a lattice-matched film. Several groups have already incorporated GaInAsN alloys into device structures which take advantage of the lower energy-gap, including fiber-optic wavelength laser diodes [4] and solar cells [5]. However, there have not yet been any reports of GaInAsN alloys with the heavy p-type doping needed for HBTs. If high p-type GaInAsN films can be grown and incorporated into the base layer of a GaAs-based HBT, it may be possible to realize microwave devices with the speeds associated with III-V materials at Si-like turn-on voltages.

While a lower turn-on voltage is the key motivation for adding N and In to the base layer of GaAs-based HBTs, a number of secondary benefits to device performance are also expected. The anticipated benefits associated with using low energy-gap GaInAsN base layers in a conventional GaAs-based HBT device structure include:

- **Lower turn-on voltage:** The addition of just 2% of N and 6% of In to GaAs can lower the energy-gap to well below that of Si (1.12 eV) and yet maintain lattice-matching to GaAs. By reducing the base layer energy-gap from 1.42 (GaAs) to 1.12 eV, the HBT turn-on voltage (V_{be} @ 100 μ A) is expected to shift from 1.12 V to 0.80 V.
- **Lower system supply voltage:** Because of the reduced turn-on voltage, circuits utilizing GaInAsN HBTs will require a lower overall system voltage. The lower system voltage enables GaAs-based power amplifier circuits to operate with the smaller batteries needed for future commercial wireless communication systems. The lower turn-on voltage will also enable better functionality in digital circuits which are currently constrained by the standard power supplies used for Si circuits. Note that this reduction in voltage eliminates one of the principal advantages of InP-based HBTs over GaAs-based HBTs [6].
- **Improved temperature stability:** The increase in collector current density associated with the reduction in turn-on voltage increases the neutral base recombination component of the base current relative to the reverse hole injection component, and thus improves the stability of the peak DC current gain.
- **Better RF performance:** GaInAsN alloys enable the implementation of several device structures, such as a graded energy-gap base, which enhance RF performance.
- **Increased reliability:** The reliability of GaInAsN HBTs may be improved over conventional GaAs HBTs due to the increased robustness of material with In and N doping (alloy hardening), increased hole confinement, and suppressed $n=2$ base current components.
- **Higher low bias DC current gain:** An increase in the collector current relative to fixed $n=2$ base current components leads to a higher DC current gain at low bias and a more stable gain as a function of current density.
- **Increased circuit design flexibility:** In addition to relaxing the constraints on power supply voltage, the lower turn-on voltage and stable gain as a function of both voltage and temperature gives circuit designers more latitude to optimize amplifier circuit parameters such as linearity and power add efficiency (PAE). A lower turn-on voltage implies that a given current can be achieved at lower bias, allowing a higher PAE to be achieved at low applied bias. Linearity may also be improved by a resulting increase in the reverse bias on the base-collector junction. In digital circuits, a lower bias voltage should reduce the power-delay products [15].
- **Reduced process sensitivity:** The impact of $n=2$ recombination processes at the emitter-base junction and the emitter periphery will be reduced due to the increased collector current. Thus GaInAsN HBTs may not require passivating ledges, reducing processing complexity and cost.

During our Phase I effort, we have demonstrated over 120 meV reduction in the energy-gap of heavily p-type GaAs ($3 \times 10^{19} \text{ cm}^{-3}$) by adding both In and N to the material. Moreover, these results have been achieved using a growth process which is compatible with high volume manufacturing. We propose to further optimize the growth process and incorporate p-type GaInAsN into the base layer of InGaP/GaAs HBTs in a Phase II effort aimed at realizing the benefits of this exciting new material system. InGaP is chosen as the emitter layer because of its low conduction band offset with GaAs and its demonstrated reliability. As outlined in the following sections, we plan an integrated effort involving both university and industrial partners to explore basic material issues, optimize growth, incorporate the new materials into HBT structures, and probe a wide range of large and small area device characteristics. The overriding goal of the proposed Phase II work is to demonstrate improved device performance in a GaAs-based material system and quickly bring the new device structures to market.

Phase I Technical Objectives

The turn-on voltage on an HBT is fundamentally limited by the energy-gap of the base layer. By utilizing p-type GaAs layers co-doped with In and N, the energy-gap of the base layer can be significantly reduced. We plan to incorporate such p-type GaInAsN layers into a GaAs-based HBT structure and demonstrate the enhanced device performance outlined in the previous section. However, GaInAsN is a new material and there are many basic issues which need to be investigated before these benefits can be realized. Kopin Corporation plans to work closely with both university and industrial partners to address these issues and explore the potential benefits of GaInAsN HBTs. As describe below, we plan to focus on optimizing the growth process, incorporating GaInAsN into an HBT structure, and probing a wide range of device characteristics in both large and small area devices. Growth optimization will focus on understanding better and refining further a proprietary growth process developed during the Phase I effort. Large area device characteristics will be heavily used to assess both the quality of the material in the full HBT structure and the success of the device design. Small area device performance will be used to determine the overall success of the project.

1.0 Optimize Growth Process for p-type GaInAsN

During our Phase I effort, we have made significant progress incorporating over $1\text{E}19\text{ cm}^{-3}$ of N into GaAs and GaInAs layers, and we have observed over a 120 meV shift downward in the energy-gap of heavily p-type GaAs. Moreover, we have achieved these results using a unique growth process which is compatible with high volume production. In a Phase II effort, we need to develop a better understanding of the growth of N containing layers in general and this growth process in particular in order to better optimize the material properties for HBT applications.

1.1 Growth of GaInAsN Alloys

Recently, there have been numerous reports concerning GaAs and related compounds doped with small amounts of N [1-3]. Such GaAsN alloys have a number of interesting properties, not least of which is a very large reduction in energy gap with the addition of small amounts of N (Figure 1). For example, recent calculations suggest that unstrained GaAsN with just 4% N will have an energy gap in excess of 200 meV lower than GaAs [7]. The reduction in energy-gap is even greater in strained-layers. Figure 1 highlights the projected energy gap of GaAsN alloys as a function of lattice constant. Because of a huge band-gap bowing parameter, the energy-gap of GaAsN first drops as N is added before it begins to increase toward the energy gap of GaN (3.4 eV) at higher N concentrations. The lattice constant of GaAsN decreases as N is added. Also highlighted in Figure 1 is the energy-gap of GaInAs alloys. As In is added to GaAs, the energy-gap also decreases, but the lattice constant increases. By adding both In and N to GaAs, the energy-gap can be dramatically reduced, but if added in the correct ratio, the lattice constant can remain near that of GaAs. Such lattice-mated GaInAsN alloys with energy-gaps as low as 1 eV have been synthesized by several groups and incorporated into both laser diodes and solar cells [4, 5].

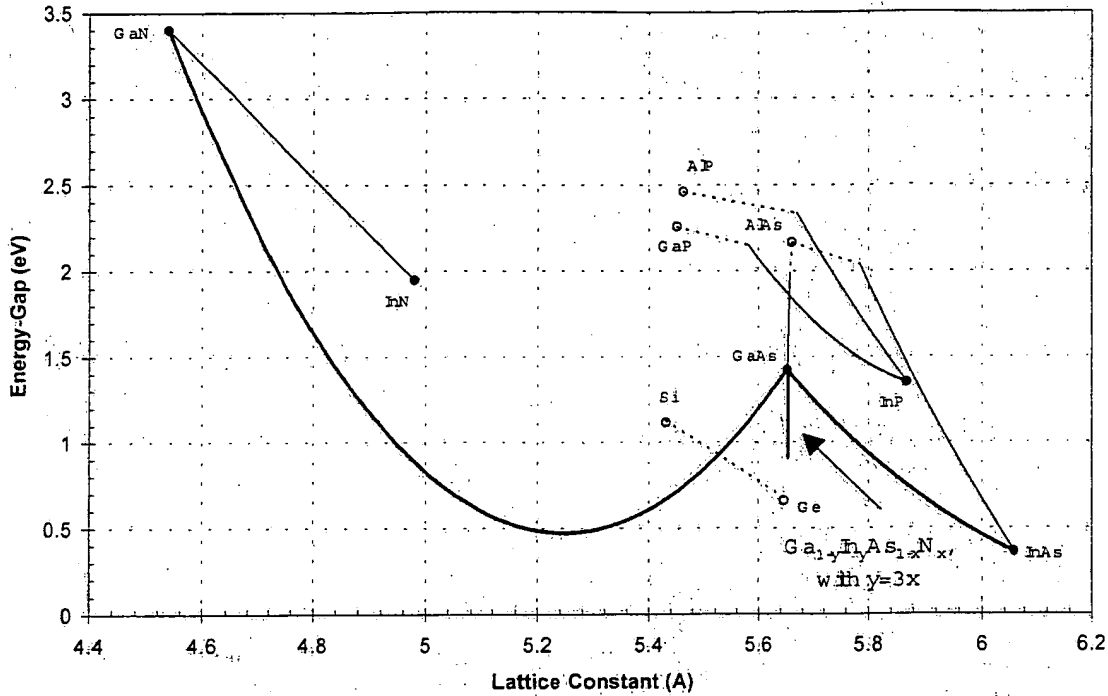


Figure 1: Energy-gap vs. lattice constant for common III-V semiconductors including GaAsN. Highlighted are the GaAsN and GaInAs ternaries, as well as the lattice-matched GaInAsN quaternary.

During our Phase I effort, we have added enough In and N to heavily p-type GaAs ($3 \times 10^{19} \text{ cm}^{-3}$) to achieve over a 120 meV downward shift in photoluminescence (PL) energy-gap at 77K. Figure 2 shows the PL spectrum from both a control sample and a film codoped with In and N. For the GaInAsN sample, the N source flow has been scaled to yield a target level of $1 \times 10^{19} \text{ cm}^{-3}$, and enough In has been added to make the film lattice matched to GaAs. The growth has also been optimized to maintain a high p-type doping level near $3 \times 10^{19} \text{ cm}^{-3}$ as measured by Hall. For a GaAs film doped p-type at standard level of $4 \times 10^{19} \text{ cm}^{-3}$, we observed a peak 77K PL wavelength of 8500 Å, as shown in Figure 2. The peak wavelength of p-type GaAs decreases with decreasing doping toward a wavelength of 8228 Å for undoped GaAs. The peak PL wavelength of the GaInAsN film in Figure 2 is shifted outward to 9273 Å. This corresponds to an energy-gap of 1.34 eV and is over 120 meV lower than our standard $4 \times 10^{19} \text{ cm}^{-3}$ p-type GaAs layers.

The GaInAsN film whose PL is shown in Figure 2 is nearly lattice matched to GaAs. When doping with carbon, as these samples are, the lattice constant of GaAs shrinks, causing the film peak in a double-crystal x-ray diffraction (DCXRD) spectrum to shift to the right of the GaAs substrate. For doping levels near the $4 \times 10^{19} \text{ cm}^{-3}$, the film DCXRD splitting is typically around +90 arcsec. Adding N shifts the peak film further to the right and thus increases the splitting. However, when In is added, the lattice constant expands, pushing the film peak to the left. Figure 3 shows the DCXRD spectrum from four GaInAsN samples with different levels of In source flow added to the growth. The

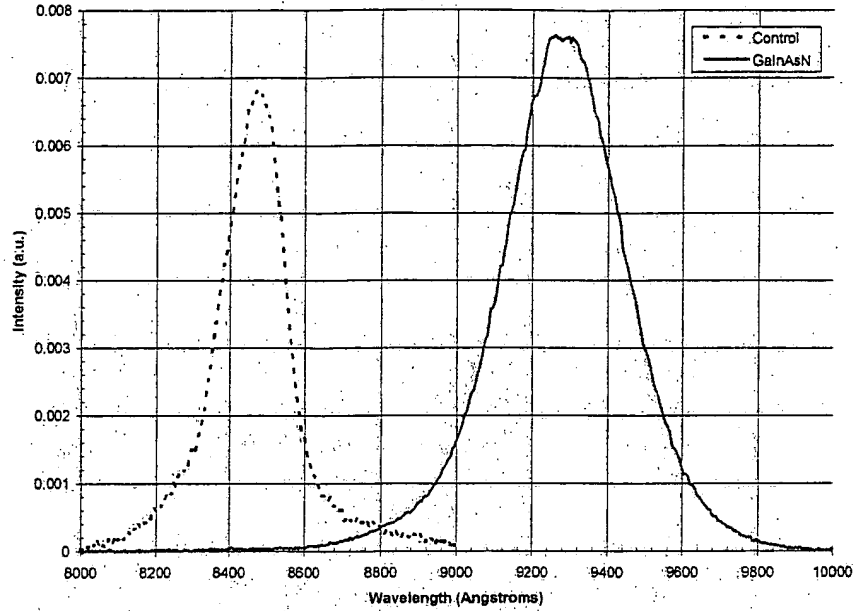


Figure 2: 77 K PL spectrum from a control p-type GaAs sample and a sample codoped with In and N. The peak wavelength shifts outward from around 8500 Å in the control to 9273 Å in the sample containing In and N. DCXRD of the GaInAsN sample indicates it is lattice matched to the GaAs substrate, and Hall gives a doping level of $3 \times 10^{19} \text{ cm}^{-3}$. Because of differences in structure and excitation power, the magnitude of the two PL intensities can not be compared.

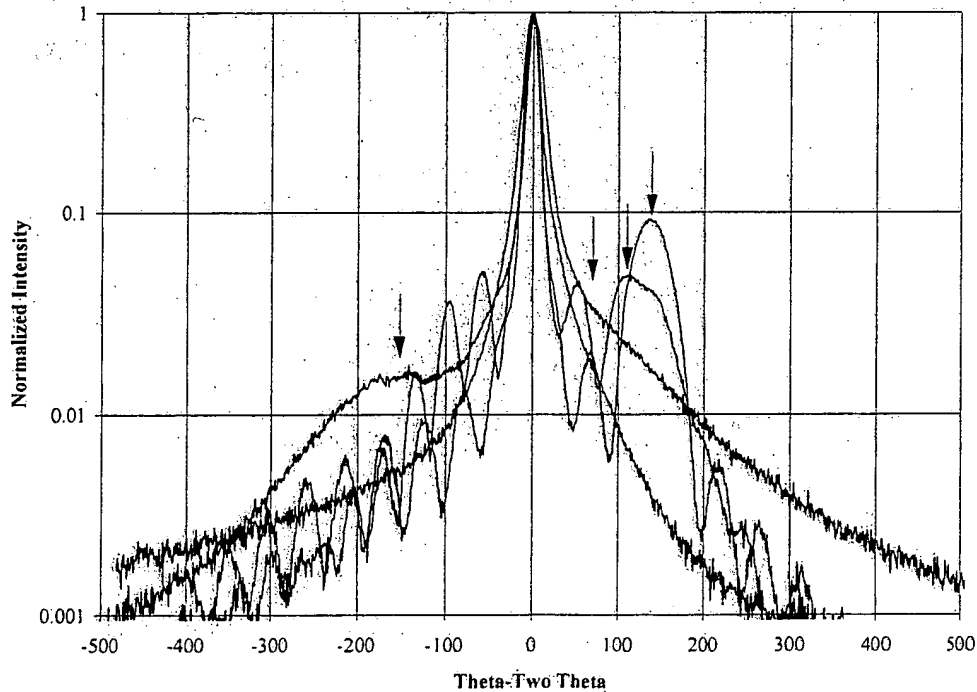


Figure 3: DCXRD of bulk (5000 Å) GaInAsN layers grown with varying In source flow. As the In source flow increases, the film peak shifts to the left (arrows).

film peak splitting moves from approximately +125 arcsec with no In flow to -60 arcsec with the highest In flow. The third In source flow, which is nearly lattice matched, was used for the growth of the GaInAsN sample whose PL is shown in Figure 2.

While we have been successful at growing GaInAsN films like a number of other groups, the growth mechanisms behind N containing GaAs-based films are not well understood. GaAsN alloys have long been predicted to have a large miscibility gap. Moreover, thermodynamic considerations suggest that N incorporation in GaAs should be quite low. However, MOCVD growth does not occur under equilibrium conditions. Kinetics, not thermodynamics will determine N incorporation. Indeed the recent reports on the properties of N in GaAs far exceed the initial theoretical predictions. In this project we plan to carefully study the impact of MOCVD growth parameters on the properties of N-doped GaAs layers. We anticipate that growth temperature, source flows, and growth chemistry will all play important roles in N incorporation.

1.2 Manufacturable Growth Process

Most recent MOCVD demonstration of GaAsN films have employed plasma or other alternative N sources [1, 3, 5, 8, 9]. Dimethylhydrazine (DMHy) has been the most popular of the alternative N sources. However, none of these alternative N sources are compatible with high volume production. DMHy in particular is both dangerous and expensive. During the Phase I effort, we have engaged in discussions with several metalorganic source vendors concerning DMHy. While they are willing to make and sell DMHy, the vendors felt it would work only as a laboratory demonstration, not as a production source. We believe ammonia (NH_3), the typical N source for GaN growth, may be a better choice. Ammonia is a very clean source that is produced in large volumes and at low price. Concerns that NH_3 does not crack sufficiently at low temperatures seem unwarranted to us. It is well known that a key step to growing high quality GaN layers on sapphire substrates involves a low temperature ($\sim 550^\circ\text{C}$) buffer layer. Since NH_3 and TMGa are the typical sources for this buffer layer, it is clear that NH_3 can be used as a N source at low growth temperatures. We feel the known benefits of using a well established source far outweigh the potential benefits of trying an alternative N source.

During the Phase I effort, we have determined that NH_3 is a suitable source for growing N-doped GaAs films, even at low temperatures. The SIMS profile of the N concentration in a $2\text{ }\mu\text{m}$ p-type GaAs film containing five layers with different N source flows is shown in Figure 4. The peak N concentration is $8.4\text{E}18\text{ cm}^{-3}$. The O and Si levels in this sample are below the detection level, while the C concentration ranges from 3.5 to $6.9\text{E}19\text{ cm}^{-3}$. Most encouraging is the plot of N concentration versus N source flow shown in Figure 5. A least squares fit indicates the N concentration is increasing linearly with N source flow and suggests that increasing the N concentration in the films is simply a matter of increasing the source flow.

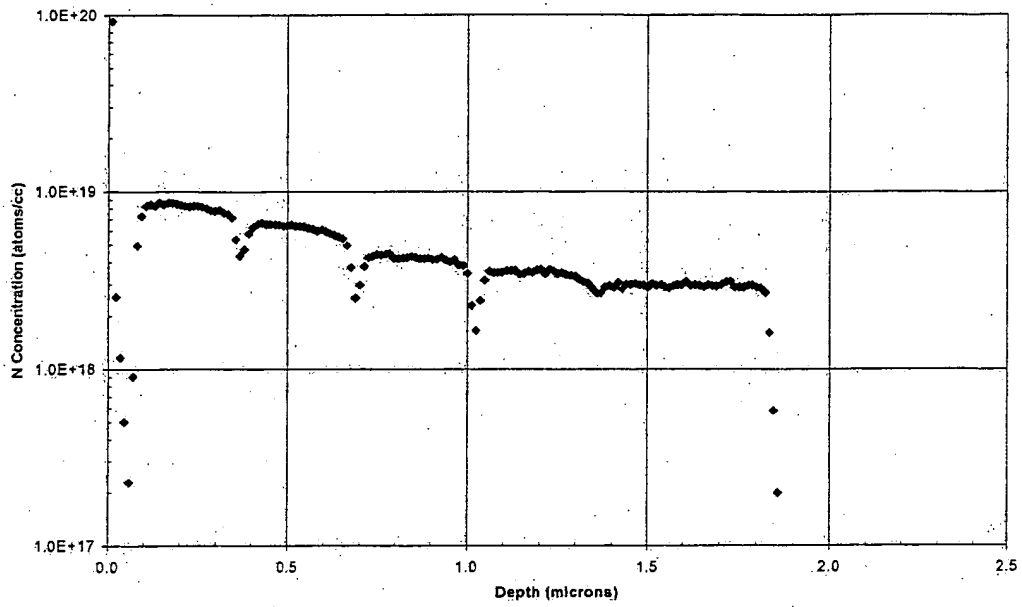


Figure 4: SIMS profile of the N concentration through a p-type GaAs sample consisting of five layers with different N source flows.

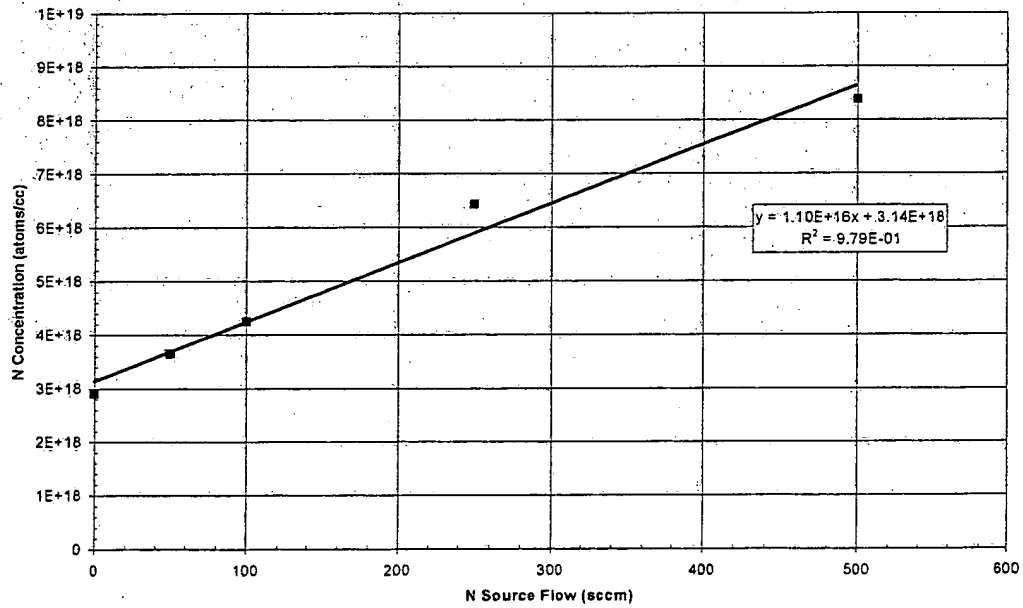


Figure 5: Average N concentration in the five layers shown in Figure 4 as a function N source flow. The solid line represents a least squares linear fit of the data.

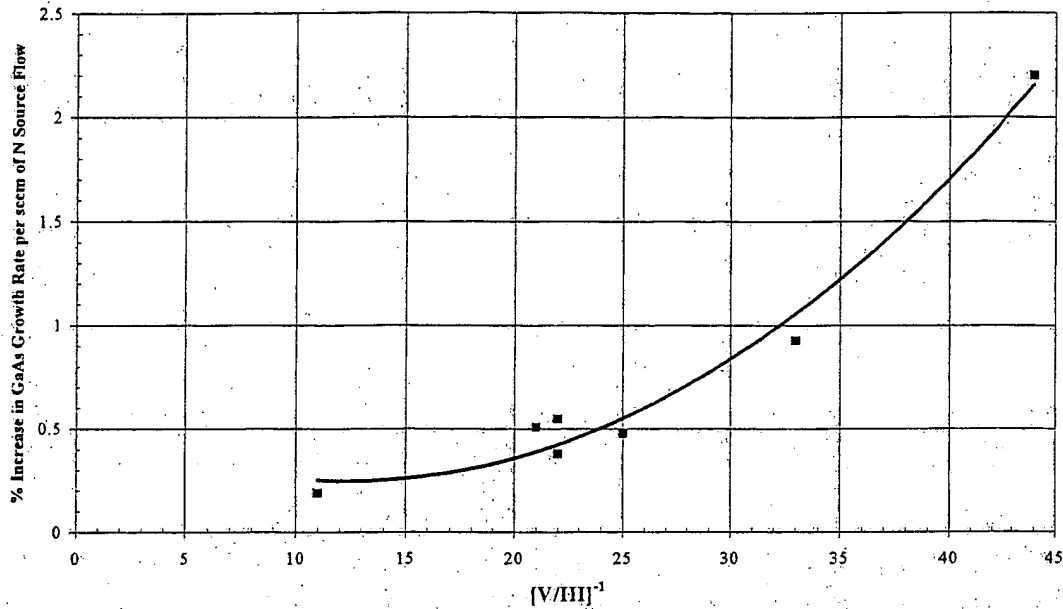


Figure 6: Effect of nitrogen source flow on GaAs growth rate as a function of arsenic and gallium source flows. The V/III gas flow ratio has been varied by changing both the gallium and arsenic source flows. The impact of N source flow on GaAs growth rate has been assumed to be linear.

While the NH_3 -based growth process developed during Phase I looks very promising, it needs to be better understood and optimized during the Phase II effort. The initial growth experiments at Kopin investigated the impact of growth temperature as well as gallium, arsenic, and nitrogen source flows. A set of single layer, bulk (5000 Å) structures were grown and characterized by Hall, selective etch, DCXRD, and PL. The results clearly indicate a complex growth chemistry with many interactive effects between the growth parameters. For example, at low nitrogen source flows, the GaAs growth rate increases with increasing nitrogen source flow. Moreover, the magnitude of this effect of nitrogen source flow on GaAs growth rate varies dramatically with the gallium and arsenic source flows. Figure 6 shows the percent increase in growth rate per sccm of nitrogen source flow as a function of inverse V/III gas flow ratio. Under some conditions, a 50 sccm nitrogen source flow can lead to over a 50% increase in the GaAs growth rate. These results suggest that the nitrogen source flow acts as a catalyst for the decomposition of gallium and arsenic sources. Since most models of the MOCVD growth of GaAs hypothesize that gallium and arsenic source molecules interact on the surface, the results summarized in Figure 6 suggest the nitrogen source may interact with both the gallium and arsenic source molecules on the growth surface and not in the gas stream.

In addition to the growth chemistry, the stability of the process needs to be optimized. Photoluminescence spectrum of thick and thin samples grown under identical conditions show very different full width half maxims (Figure 7). The PL from the thicker sample is considerably broader and the peak is shifted outward to a longer wavelength. SIMS profiles through the thicker sample indicate that the N and C concentrations are drifting during growth (Figure 8).

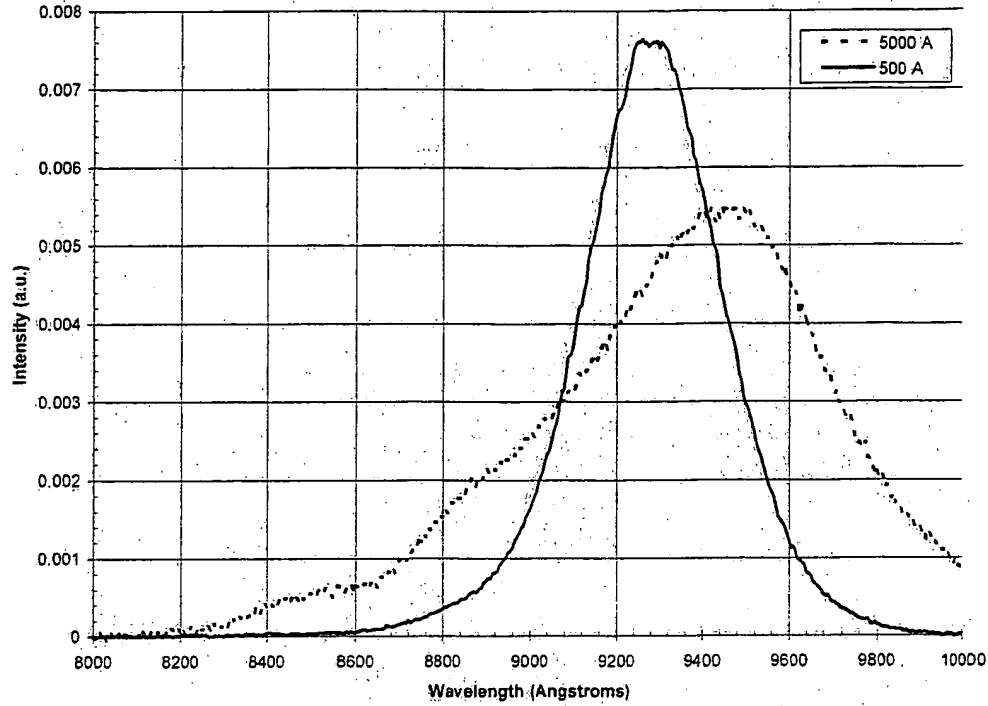


Figure 7: 77 K PL spectrum from a thin (~ 500 Å) and thick (~ 5000 Å) p-type GaAs samples codoped with In and N. The peak wavelength shifts outward from around 9273 Å in the thin sample to 9456 Å in the thick sample, and the FWHM increases from 374 Å to 609 Å.

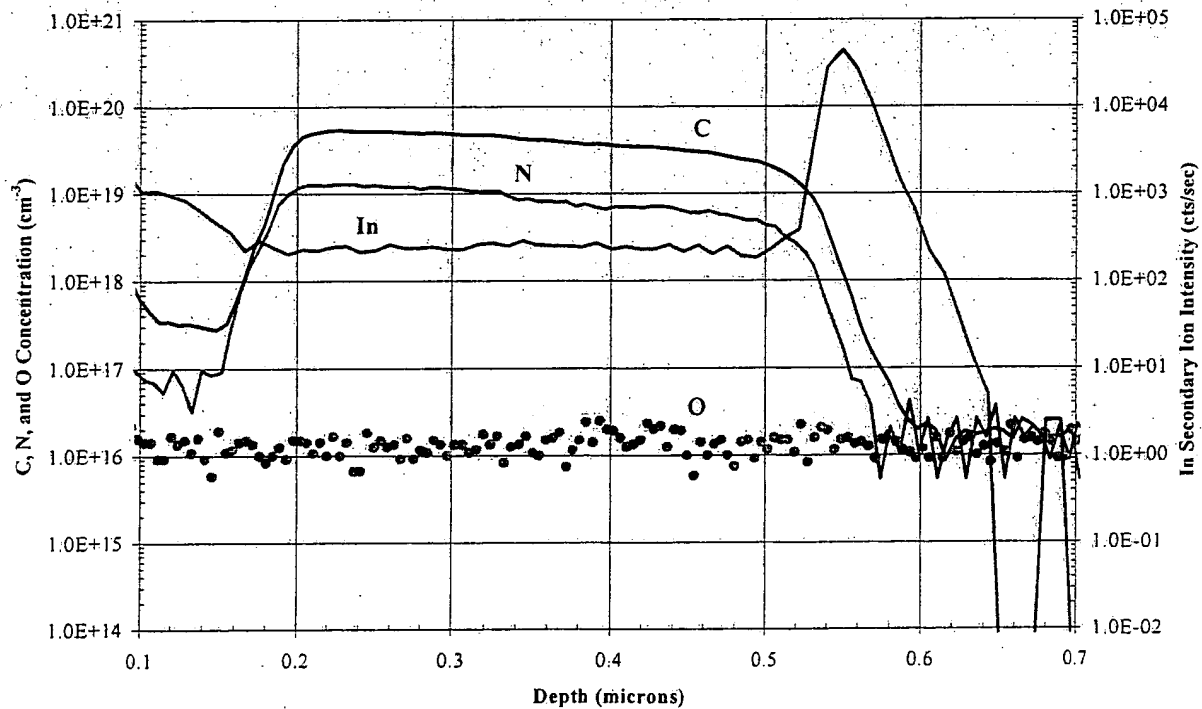


Figure 8: SIMS of the thick (~ 5000 Å) p-type GaAs sample codoped with In and N shown above in Figure 7.

1.3 Bulk p-type GaInAsN Material Properties: Energy-gap, Minority Carrier Lifetime, and Doping

As demonstrated by the PL spectrum shown in Figure 2, we have proven the feasibility of growing p-type GaInAsN with a measurable shift in energy-gap and a reasonable PL intensity during our Phase I effort. In a Phase II effort, we intend to further lower the energy-gap, increase the minority carrier lifetime (i.e. PL intensity) and maintain a high p-type doping. Carbon is the dopant of choice in modern GaAs-based HBTs because of its low diffusivity. Any potential advantages of using GaInAsN alloys for HBTs must be accomplished in films which are co-doped with C. Although C, As, and N all share the same sublattice site, we do not expect competition for the group V site to be a major obstacle to achieving co-doped films. It is already well known that C can be incorporated in large quantities in both GaAs and GaN [10]. Growth chemistry, however, can play a role in hindering C incorporation in GaAs-based alloys in some cases. Historically, it has been very difficult to grow carbon-doped GaInAs using TMIn. Experiments conducted during the Phase I effort suggest the addition of NH_3 helps offset the reduction in carbon with increasing TMIn flow. SIMS analysis of our N-containing samples indicate the C levels are well above $4 \times 10^{19} \text{ cm}^{-3}$. The objective of the Phase II work will be to optimize the growth conditions to maintain both high C concentration and a high percentage of electrical activation of the C.

We made dramatic improvements in the minority carrier lifetime of N-containing layers as measured by PL over the initial months of the Phase I effort. Rather simple modifications of the bulk structure and the growth conditions employed resulted in a two orders of magnitude increase in the PL intensity. When care is taken to match both structure and excitation power, PL intensities of GaInAsN layers are within a factor of 5 of standard p-type GaAs samples. During Phase II, we plan to further improve these results.

We have demonstrated over a 120 meV reduction in the energy-gap of heavily p-type GaAs layers during our initial Phase I work by incorporating both In and N. During our Phase II work, we will attempt to increase the magnitude of this energy-gap reduction. Based upon published literature, it should be possible to reduce the energy-gap over 400 meV. As discussed further in the next section, any decrease in energy-gap can lower the turn-on voltage of an HBT. The technical challenge will be to further lower the energy-gap while maintaining a high doping level and minority carrier lifetime.

2.0 Incorporate p-type GaInAsN Layer in an HBT

While the growth of high quality p-type films is necessary for high performance HBTs, it is not sufficient. The p-type GaInAsN films must also be successfully incorporated into a full HBT structure. Interfaces between the base and the collector and the base and emitter layers must be perfected. The design of the device structure is also critical for realizing improved device performance. Large area device results will be used as a critical characterization tool to assess material quality and device design.

2.1 Device Design

The basic device structure to be used for exploring the impact of N-doping on GaAs HBTs is shown in Figure 9. The structure consists of a GaAs buffer layer, Si-doped GaAs subcollector and collector layers, a 700 Å C-doped GaInAsN base layer, a wide band gap InGaP emitter, and GaAs and InGaAs emitter contact layers. As discussed further in the next section, the use of a wide energy-gap emitter is critical for achieving state-of-the-art device performance. While GaAs emitters could be used to demonstrate HBT devices with a GaInAsN base at a laboratory level, the lower energy-gap of GaAs relative to AlGaAs or InGaP will seriously compromise device performance, making the devices unsuitable for real life applications. InGaP is chosen for the emitter layer over AlGaAs because of its lower conduction band discontinuity with GaAs. It is much easier to eliminate the impact of the conduction band spike on collector current using InGaP in the emitter of GaAs-based HBTs. As the energy-gap of the base layer is reduced using GaInAsN, the conduction band spike will become more of a problem limiting collector current at both the emitter-base and collector-base interfaces. Thin transitional layers on both sides of the base layer are built into the basic device structure shown in Figure 9 to control the conduction band spike problem.

The importance of controlling the conduction band spike to achieve the lowest possible turn-on voltage is illustrated in Figure 10. Figure 10 depicts the Gummel plots of two 35% $\text{Al}_{0.35}\text{Ga}_{0.65}\text{As}/\text{GaAs}$ HBTs and an InGaP HBT. In one of the $\text{Al}_{0.35}\text{Ga}_{0.65}\text{As}/\text{GaAs}$ HBTs, the emitter-base interface is unoptimized. In this case, a large conduction band spike at the base-emitter interface drastically reduces the collector current. In the other $\text{Al}_{0.35}\text{Ga}_{0.65}\text{As}/\text{GaAs}$ HBT, the emitter-base interface is optimized, and the collector current has been increased by an order of magnitude. Note this reduction in the base-emitter interface has been achieved without sacrificing other device characteristics such as the low bias base current. The collector current of the optimized $\text{Al}_{0.35}\text{Ga}_{0.65}\text{As}/\text{GaAs}$ HBTs overlays the collector current of an InGaP/GaAs HBT with the same base sheet resistance. The collector current of these devices is limited by the energy-gap of GaAs.

The use of GaInAsN base layers in GaAs-based HBTs also enables more advanced device structures. Graded-base HBTs have long been advocated as a device design beneficial for improving the RF performance of HBTs [11]. A graded base introduces a quasielectric field which reduces the base transit time. Specifically, the quasielectric field adds a drift component to minority carrier transport which pushes electrons towards the collector in a npn HBT (Figure 11). Thus, for a fixed base thickness and doping level (yielding a desirably low base sheet

500 Å Si-doped $\text{In}_{0.6}\text{Ga}_{0.4}\text{As}$ ($1 \times 10^{19} \text{ cm}^{-3}$)
500 Å Si-doped InGaAs Grade ($1 \times 10^{19} \text{ cm}^{-3}$)
1500 Å Si-doped GaAs ($5 \times 10^{18} \text{ cm}^{-3}$)
450 Å Si-doped InGaP ($3 \times 10^{17} \text{ cm}^{-3}$)
50 Å Si-doped InGaP/GaAs Transitional Layer
700 Å C-doped $\text{Ga}_{1-y}\text{In}_y\text{As}_{1-x}\text{N}_x$ ($4 \times 10^{19} \text{ cm}^{-3}$) $y \approx 3x$
500 Å Si-doped GaAs Transitional Layer
7000 Å Si-doped GaAs ($1 \times 10^{16} \text{ cm}^{-3}$)
5000 Å Si-doped GaAs ($5 \times 10^{18} \text{ cm}^{-3}$)
500 Å undoped GaAs
GaAs SUBSTRATE

Figure 9: Schematic of proposed GaAs-based HBT using a lattice-matched GaInAsN base.

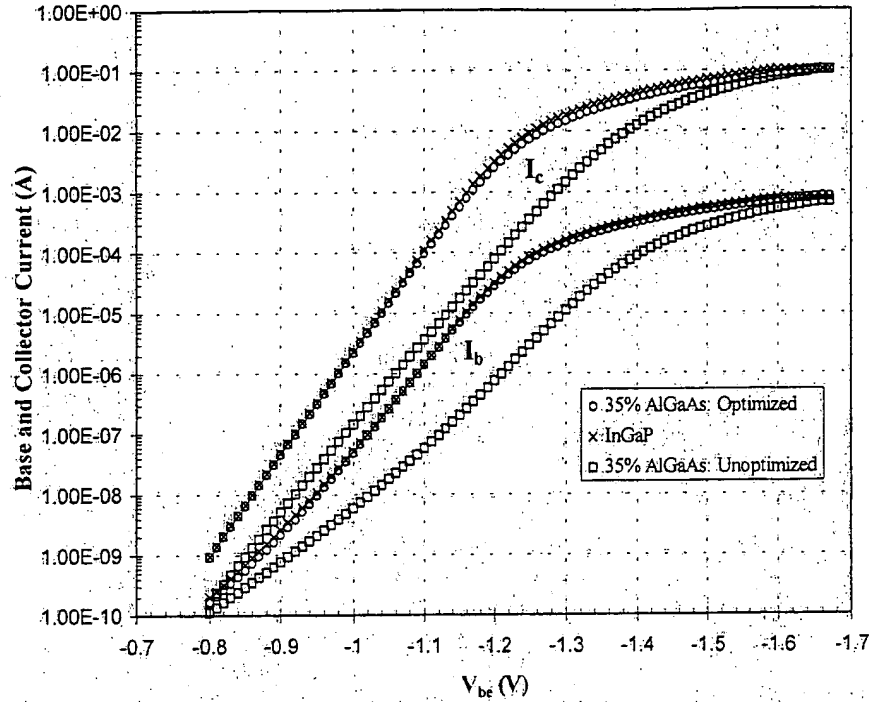


Figure 10: Gummel plots from large area devices ($75\ \mu\text{m} \times 75\ \mu\text{m}$) on three samples with different emitter structures and $4E19\ \text{cm}^{-3}$ base layers ($R_s\text{base} \sim 250\ \text{Ohms/Square}$). The collector current of the unoptimized 35% AlGaAs structures is almost an order of magnitude lower than in the optimized 35% AlGaAs and InGaP emitter structures. The base current of the three emitter structures is comparable at low bias, but the base current of the 35% AlGaAs emitter structure is lower at high bias. The base current follows the collector current at high bias where neutral base recombination dominates.

resistance), the base transit time can be increased by using a graded base. The enhanced performance of such graded-base structures has been demonstrated experimentally [12]. However, this device design has not been widely implemented because of several material problems. Using AlGaAs to grade the base layer energy-gap reduces hole confinement and tends to lower material quality relative to GaAs, which can seriously hamper the initial performance and the long-term reliability of an HBT. Graded GaInAs base layers introduce strain into the device structure which limits the amount of energy-gap grading that can be implemented. The difficulty in achieving high p-type doping in GaInAs using C as the dopant has also seriously limited the application of graded-base structures. By ramping both the In and N concentration, GaInAsN could be used to grade the base layer without introducing strain into the device. As discussed earlier, we have been able to grow GaInAsN films with high C levels during our Phase I work. Alternatively, In-free GaAsN layers could be used to grade the base. While this introduces strain, the energy-gap of GaAsN falls much more rapidly than GaInAs for a given level of lattice-mismatch. Our calculations suggest that a graded GaAsN base layer with significant energy-gap grading could be grown while keeping the critical thickness above $700\ \text{\AA}$, a typical base layer thickness for GaAs-based HBTs.

A number of possible additional benefits could arise from using GaAsN alloys in the base of GaAs-based HBTs. Strained GaAsN HBTs open up the possibility of a device design not available with strained InGaAs HBTs. When a strained layer is grown on certain axes, such as the (111)B orientation, the strained layer gives rise to a piezoelectric field [13]. Like in a graded base structure, the field produced by the piezoelectric effect can be used to accelerate minority carriers across the base layer. However, in an HBT with an InGaAs base in a standard emitter-up configuration, the piezoelectric field actually opposes electron transport to the collector. Since GaAsN is tensively strained to GaAs instead of compressively strained, the piezoelectric field is reversed, and electron transport is enhanced. Thus the same advantages of the graded-base structure could be achieved by growing a simple uniform GaAsN base on a (111)B GaAs substrate.

In addition to enhanced RF performance, GaAs-HBTs employing a graded-base structure can improve the overall characteristics of small area devices. GaAs is well known to have large surface recombination due to a large density of surface states which pin the Fermi-energy near the mid-gap. As device area decreases, parasitic currents (due to the loss of carriers at the surface of the base layer exposed around the device periphery during processing) can degrade performance. To overcome this problem, GaAs-based HBTs typically employ a "ledge" of passivating material around the perimeter of the device as shown in Figure 12. However, it has also been shown that structures with a built-in electric field in the base can also improve small area device performance without the use of a ledge [14]. The electric field accelerates minority carriers away from the top of the base and into the collector. Since the Fermi-level of a GaN surface is reported to be unpinned, the addition of N to the base of a strained or graded-base HBT may further reduce surface recombination effects. We envision that the use of a less complex "ledgeless" HBT process will lower chip cost.

The high mobility and electron velocities of GaInAs are employed in InP-based HBTs to decrease the transit time through the collector layer and enhance RF performance. Similar benefits could be achieved in GaAs-based HBTs by incorporating In into the collector, but strain effects seriously limit the implementation of this device design. The electronic properties of n-type GaInAsN are unknown at this time. However if these films offer any of the electronic advantages of GaInAs over GaAs, implementation into an HBT structure would be straight forward due to the lattice matching enabled by the addition of N to GaInAs.

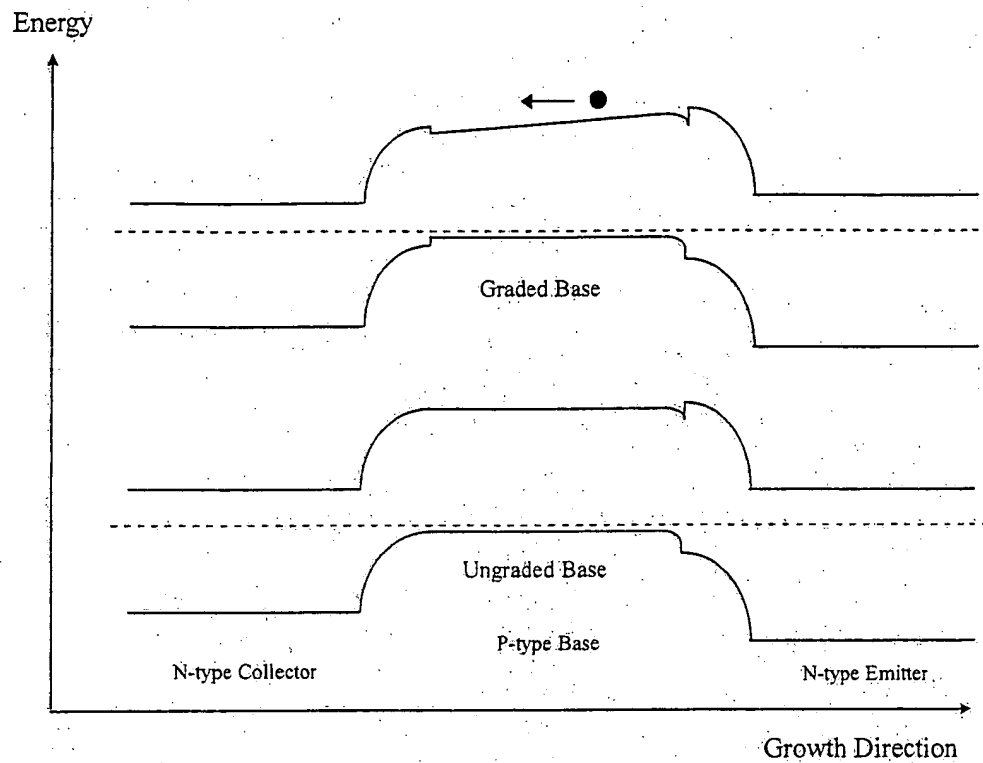


Figure 11: Comparison of the unbiased energy-gap versus position diagrams of (a) graded-base and (b) uniform base HBTs.

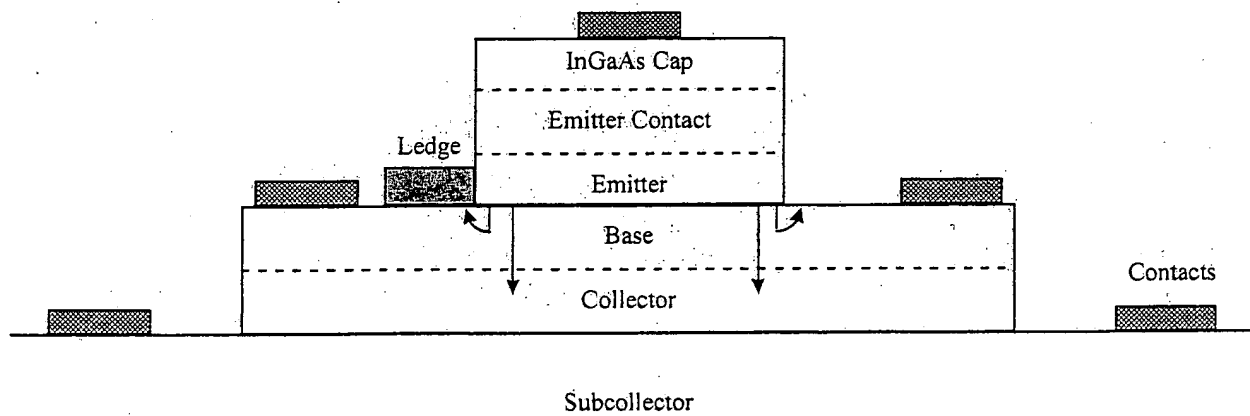


Figure 12: Representative cross-section of a small area HBT in which the left side of the emitter mesa employs a passivating ledge but the right side does not.

2.2 Large Area Device Analysis

At Kopin, we rely heavily on using the characteristics of large area HBTs to assess the properties of the epitaxial layers. After examining large area device characteristics from a great number of structures grown under a fairly wide range of conditions, we have learned a good deal about the relationship between material properties and device characteristics. By analyzing the Gummel plots of a device, we can gauge the quality of the base layer, the nature of the emitter-base interface, and the properties of the wide energy-gap emitter. Below we describe the basics of a model we use to help analyze device results and relate this model to the enhancements in device performance that we expect to see when the energy-gap of the base layer is reduced.

If the collector current of an HBT is governed just by simple diffusion of carriers across the emitter-base junction, the collector current density (J_c) could be expressed as:

$$J_c = (qn_i^2 D_n / p_b w_b) \exp(qV_{be}/kT)$$

where n_i is the intrinsic carrier concentration in the base, D_n is the electron diffusivity, and p_b and w_b are doping and thickness of the base layer [15]. Solving for V_{be} we get

$$V_{be} = (kT/q) \ln[p_b w_b J_c / qn_i^2 D_n].$$

Typically, we define the turn-on voltage to be the V_{be} at which the collector current reaches a fixed value (1E-4 A on a 75 μm x 75 μm device = 1.78 A/cm²). Remembering that the base sheet resistance ($R_s\text{base}$) is defined as:

$$R_s\text{base} = [qp_b w_b]^{-1},$$

and that the intrinsic doping level can be related to the base layer energy-gap (E_{gb})

$$n_i^2 = N_c N_v \exp(-E_{gb}/kT),$$

where N_c and N_v are the effective density of states in the conduction and valence bands in the base layer, then the above expression for V_{be} can be related to $R_s\text{base}$:

$$V_{be} = E_{gb}/q - (kT/q) \ln[q^2 \mu N_c N_v D_n / J_c] - (kT/q) \ln[R_s\text{base}].$$

In practice, the collector current is frequently limited by a conduction band spike at the base-emitter interface which causes the V_{be} to be higher than in the diffusive limit describe above. Figure 13 shows the variation in turn-on voltage ($V_{be}@J_c=1.78 \text{ A/cm}^2$) with $R_s\text{base}$ from both unoptimized AlGaAs and InGaP HBTs. The V_{be} of the InGaP HBTs nicely follows the natural logarithm dependence on $R_s\text{base}$ described above, while the V_{be} from the AlGaAs HBTs is higher and does not fit the natural logarithm dependence as well. Examination of the reverse Gummel plots from these devices indicate that the conduction band spike is limiting the collector current in the AlGaAs samples but not in the InGaP samples. Also shown in Figure 13 is the expected V_{be} dependencies in the diffusive limit as the base layer energy-gap is lowered in 50 meV increments.

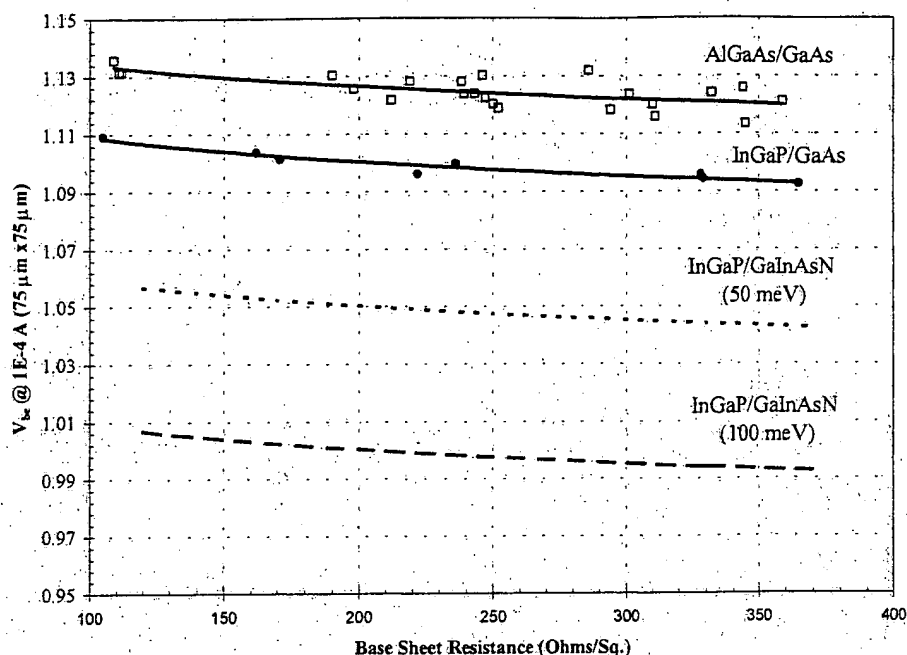


Figure 13: Turn-on voltage as a function of base sheet resistance for unoptimized AlGaAs/GaAs HBTs (squares) and InGaP/GaAs HBTs (circles). Also shown are least squares fits of the data using a logarithmic function (see text), as well as the expected V_{be} of InGaP/GaInAsN HBTs in which the energy-gap of the GaInAsN base layer is 50 and 100 meV below that of GaAs.

The base current of a large area GaAs-based HBT is composed of several different components, including space charge recombination, neutral base recombination, and reverse hole injection [15]. Each of these components has a physically different origin. Space charge recombination is a so called $n=2$ process which occurs predominately within the emitter layer when the base is heavily doped, and is dependent mainly on the energy gap and trap density in the emitter layer. The neutral base recombination component is proportional to the collector current via base thickness, minority carrier lifetime, and average electron velocity [16]. Reverse hole injection is an $n=1$ process and is related to the energy-gap of the emitter and the doping levels in the emitter and base layers. The relative magnitude of the three base current components as a function of bias in a typical GaAs-based device is depicted in Figure 14. The circles illustrate the collector and base currents from a high gain GaAs-based HBT with a 25% AlGaAs emitter and a base sheet resistance of $330 \Omega/\square$. The solid lines overlaying the device results illustrate the relatively good fit of the device model discussed above. The dashed lines are from the three separate components of the base current used in the model. At low bias, in Region I, the base current is dominated by space charge recombination. In Region II, both space charge recombination and neutral base recombination contribute nearly equally to the total base current. At high bias, in Region III, neutral base recombination dominates. Under some circumstances, when the neutral base recombination component is small or the hole injection component large, hole injection can cause an increase in the overall base current at high bias where self-heating is significant (Region IV).

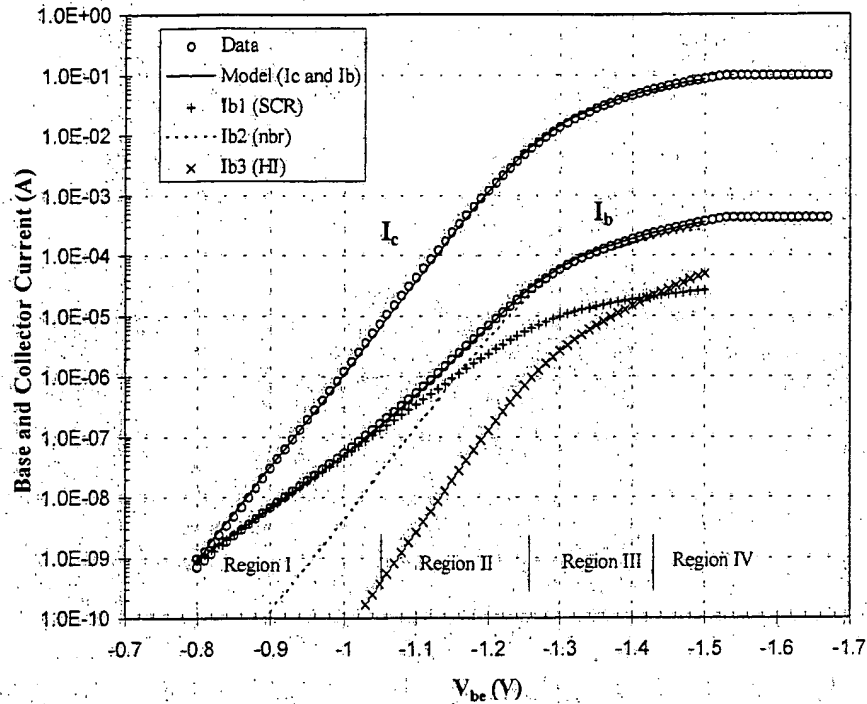


Figure 14: Gummel plot and model results for a representative GaAs-based HBT taken from a large area device ($75\ \mu\text{m} \times 75\ \mu\text{m}$) on a $\text{Al}_{0.25}\text{Ga}_{0.75}\text{As}/\text{GaAs}$ HBT wafer in which the base doping ($4\text{E}19\ \text{cm}^{-3}$) and thickness ($500\ \text{\AA}$) were calibrated to give a target base sheet resistance of $350\ \Omega/\square$.

To determine the impact of lowering the energy-gap on the DC characteristics of the HBT, we have modeled the projected Gummel plot of a GaInAsN HBT based upon our experience with GaAs-based HBTs. Shown in Figure 15 is a fit of the collector and base currents from a typical $\text{AlGaAs}/\text{GaAs}$ HBT. The collector current is fit by the exponential part of the diode equation, and the base current is fit by the three components discussed earlier. We have found this simple approach does an excellent job of fitting our observed results on both $\text{AlGaAs}/\text{GaAs}$ and InGaP/GaAs HBTs, and the turn-on voltage (V_{be} @ $100\ \text{mA}$) is typically around $1.12\ \text{V}$. The circles in Figure 15 represent model results using the same parameters needed to fit the standard $\text{AlGaAs}/\text{GaAs}$ HBT except that the energy gap of the base layer has been reduced to $1.12\ \text{eV}$. The turn-on voltage is now $0.80\ \text{V}$. Figure 16 shows the same data as Figure 15 except plotted as DC current gain versus collector current density. Unlike the GaAs HBT, the GaInAsN HBT is projected to have a nearly constant gain vs. current density. This arises because the space-charge recombination component of the base current has been reduced relative to the neutral base component. The temperature stability is also improved because the neutral base recombination component has been increased relative to reverse hole injection. As a result, the gain does not rollover at high current density with the GaInAsN base as it does for the standard GaAs-based device.

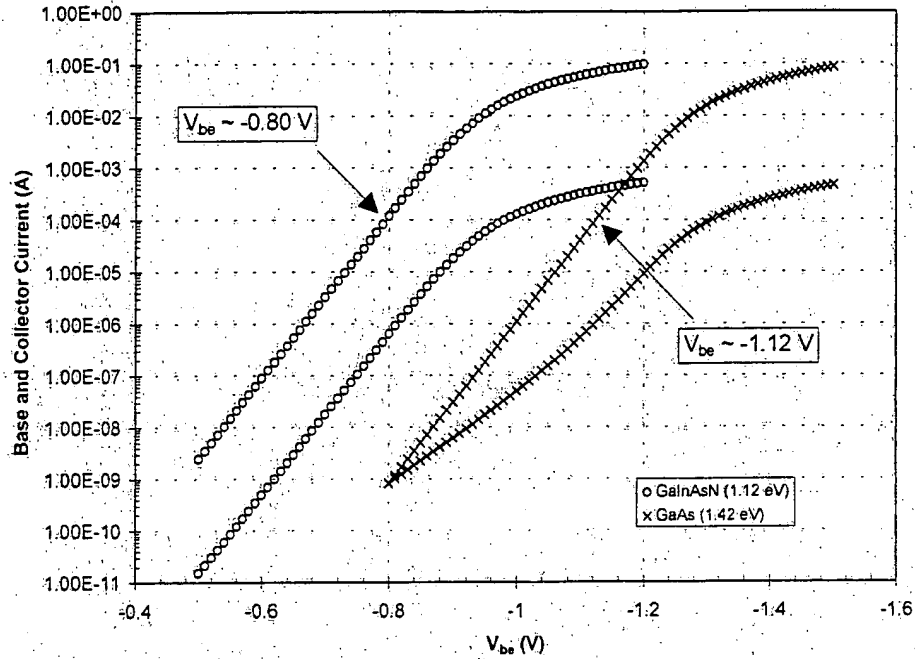


Figure 15: Projected Gummel plot of an HBT incorporating a GaInAsN base layer with an energy-gap of 1.12 eV compared to a typical AlGaAs/GaAs HBT. All device model parameters were kept fixed in the projected GaInAsN Gummel plot except the base energy-gap.

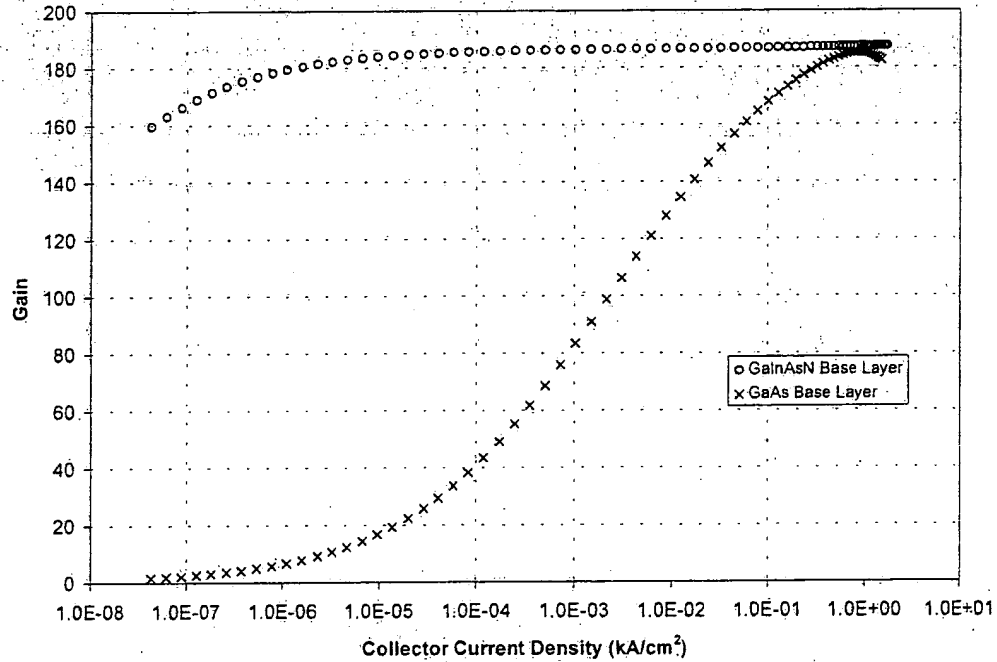


Figure 16: DC current gain as a function of collector current density extracted from the Gummel plots shown above in Figure 15. The GaInAsN-base structure has a more stable gain and does not exhibit the gain rollover typically seen in $\text{Al}_{0.25}\text{Ga}_{0.75}\text{As}/\text{GaAs}$ HBTs.

2.3 Optimize Interfaces

While the growth of high quality p-type films is necessary for high performance HBTs, it is not sufficient. The p-type films must also be successfully incorporated into a full HBT structure. Interfaces between the base and the collector and the base and emitter layers must be perfected. In addition to the differences in chemistry between the N-doped base layer and the emitter or collector layers, strain could be an issue. This strain can be eliminated by incorporating the correct ratio of In, N, and C. However, the effects of residual strain between the base, emitter, and collector layers may need to be addressed. During our Phase I effort, we have some evidence which suggest that N may be incorporated into the emitter layer grown above a N-containing base layer. At this point, the source of this unwanted N is unclear. It could be due to residual source gas which is not swept out of the growth chamber, or due to strain-induced solid-state diffusion "pulling" the N out of the base and into the emitter. During Phase II work we will conduct experiments to determine the source of the N and optimize the growth of the overlying emitter and emitter contact layers.

3.0 Demonstrate Small Area Device Characteristics

While large area device results can be used to evaluate the material properties and some aspects of the device structure, small area devices must be fabricated to ultimately determine pertinent device parameters critical for circuit performance - namely DC properties, RF characteristics, and long-term device reliability. Fabrication of small area devices is complicated for GaAs-based HBTs by the need to passivate the edges of the emitter mesa where recombination currents can be large. However, small area devices are necessary for realizing high frequency circuits.

3.1 DC Properties

The DC properties of small area devices can differ from large area devices in several important ways. Base current components originating in the perimeter region around the emitter mesa which have negligible effects on large area devices can be dominant components in small area devices. Also, small area devices can be driven to much higher current densities. It will be important to demonstrate a decrease in the turn-on V_{be} voltage not only at the relatively low current densities probed by large area devices, but also at the higher current densities found in the small area devices necessary for building microwave/millimeterwave circuits.

The temperature stability of the DC current gain is another important parameter effecting both analog and digital circuit performance. The peak DC current gain of standard GaAs-based HBTs drops with increasing temperature. This decrease in DC current gain can be modeled as resulting from an increase in the hole injection relative to other base current components such as neutral base recombination [17]. As discussed earlier, the increase in collector current resulting from a lower base energy-gap will increase the neutral base recombination component of the base current and effectively suppress reverse hole injection. As a result, we anticipate the temperature stability of the peak DC current gain to improve by using GaInAsN in the base layer of a GaAs-based HBT.

3.2 RF Characteristics

The cutoff frequency (f_t) of GaAs-based HBTs is largely governed by the transit time through the base layer and through the space charge region of the collector [18]. As discussed in section 2.1, the use of a GaInAsN base layer enables several device structures which can shorten the base transit time. The use of a standard base structure is not expected to adversely effect f_t . If incorporated into the collector layer, n-type GaInAsN may impact f_t by lowering the transit time through the collector space charge region. By maintaining a high base doping level and hence a low base sheet resistance, the maximum frequency of operation (f_{max}) can also be optimized. Together f_t and f_{max} will largely characterize the high frequency performance of an InGaP/GaInAsN transistor.

3.3 Reliability

While device reliability is a complex problem, improving reliability is of fundamental importance for gaining a wider acceptance of HBTs. GaN's extraordinary robustness to defect densities, as seen in the high brightness of blue LEDs with a 10^{11} cm⁻² dislocation density, suggests devices with N containing films may not be as sensitive to defects as traditional III-V materials [19]. More importantly, N doping in GaAs has been predicted to enhance dislocation pinning. Adding In to the active region of lasers has previously been shown to result in long-lived devices [20]. This surprising result was attributed at least in part to dislocation pinning by the In-doped GaAs. The same paper predicting the dislocation pinning properties of In-doping points out that N would be an even better dopant [21]. N-doping as a method for enhancing dislocation pinning to improve device reliability was not advocated at the time because N-doped GaAs has only been demonstrated in very recent years. This Phase II project provides one of the first opportunities to explore this phenomena.

From recent studies comparing AlGaAs- and InGaP-based HBTs, we suspect hole confinement may play a role in increasing device reliability [22, 23]. In both AlGaAs and InGaP emitter structures, the limiting factor controlling reliability appears to be an increase in the n=2 components of the base current. It is speculated that hole recombination in the emitter-base space charge region generates traps, leading to the increase in base current. While the conduction and valance band offsets between GaInAsN and InGaP are not well known, the larger energy-gap difference between a GaInAsN base and an InGaP emitter could possibly be engineered to increase hole confinement. In any event, the relative importance of all n=2 base current components will be effectively suppressed by the increase in collector current resulting from a smaller energy-gap GaInAsN base.

BEST AVAILABLE COPY